Effects of Intrauterine Alcohol Exposure on Three-Week-Old *Sprague-Dawley* Rat Distal Tibia: An Immunohistochemistry and Three-Dimensional Micro-Focus X-Ray Computed Tomography (3d-µCT) Investigation

Bello Nura Kaura

(1332538)

A Dissertation submitted to the Faculty of Health Sciences, University of the Witwatersrand, Johannesburg, in fulfilment of the requirements for the degree of Master of Science in Medicine

Johannesburg, 2018

DECLARATION

I, Bello Nura Kaura hereby declare that this dissertation is my own work, except where acknowledgement indicate otherwise. It is being submitted for the degree of Master of Science in Medicine in the Faculty of Health Sciences in the University of the Witwatersrand, Johannesburg. It has not been submitted before for any degree or examination at this or any other University. All procedures used in this dissertation were approved by the Animal Ethics Screening Committee of the University of the Witwatersrand. Ethical clearance number is AESC 2015/27/15C.

I empower the University to reproduce for the purpose of research either whole or any portion of the contents in any way whatsoever.

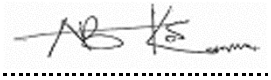

Bello Nura Kaura

Signed on 15th May, 2018

Dedicated to the loving memory of my late father

Alhaji Abubakar Bamuche (Harkar Sutura)

(1926-2016)

May his gentle soul rest in Jannah, Ameen.

ABSTRACT

Children exposed to alcohol during gestation are at risk of developing a spectrum of neurodevelopmental disorders known as fetal alcohol spectrum disorders (FASD). The most severe form of this disorder is fetal alcohol syndrome (FAS), which is characterised by neurological deficits, facial dysmorphogenesis and growth retardation. Most research is on neurological deficits and facial dysmorphogenesis, with less attention given to the effects of gestational alcohol exposure on the skeletal system. Therefore, this study investigated the effects of prenatal alcohol exposure on bone growth and development in a postnatal three week old *Sprague-Dawley* rats tibia using immunohistochemical and three dimensional microfocus x-ray computed tomography (µCT) investigations.

Female *Sprague-Dawley* rats (n=15) were time-mated and divided in to three groups as follows: (i) the ethanol group (n=6) received 0.015 ml/g body weight of 25.2% alcohol for 19 days, (ii) the saline control group (n=6) received the same dose of 0.9% saline for the same period and (iii) the untreated control group (n=3) received neither ethanol nor saline. Two Pups (n=30) from each dam (n=30} were randomly selected and terminated on day 21 after delivery and bilateral tibiae (n=60) were dissected, fixed, decalcified, processed and then subjected to histological and immunohistochemistry staining as well as µCT.

The growth plate surface area was significantly smaller with fewer cell number in proliferative and hypertrophic zones in the ethanol group. There were also fewer Ki-67 labelled cells recorded in the ethanol group. However, the full and shaft length of the

tibia were similar among all three groups in the study. We found both lower bone volume to total volume (BV/TV) and trabecular thickness (TbTh) to be lower in the ethanol group in comparison with the controls. The trabecular number (TbN) was not affected in our study. However, there was more trabecular spacing in the ethanol group.

This, considered together with the lower BV/TV and TbTh suggests that, although the bone length was similar in all groups, the internal morphology was not the same among the study groups. This indicates that prenatal alcohol exposure at our dosage may affect internal architecture while sparing the external bone length. This disruption of the internal bone morphology may also explain why FAS children are prone to osteoporosis and fracture as they may have less bony material internally.

Employing a binary logistic regression showed that the distal medullary canal area and trabecular spacing were the main parameters that determined group membership into either ethanol treated or saline control. This means that these two are affected the most in gestational alcohol exposure.

Our finding of a positive correlation between medullary canal area and cortical thickness indicates that the smaller medullary canal was coupled with thinner cortical bone. We propose that this may potentially explain weaker bones observed in FAS children.

In the ethanol group, trabecular thickness and spacing had negative loadings to the principal component analysis model. These two parameters were also negatively correlated. This suggests that trabecular formation may have been delayed in the ethanol group.

Gestational alcohol exposure had an adverse effect on the growth plate with respect to its general size, respective zone sizes and the number of cells in each zone. This may be how diminished stature of the offspring occurs. Fewer proliferative cells were found using the anti-Ki67 antibody, indicating that in utero alcohol exposure slows cell proliferation, contributing to the small stature.

Logistic regression showed that the distal medullary canal area and trabecular separation were the main parameters affected the most in gestational alcohol. The negative correlation of trabecular thickness and spacing in the ethanol group may be a contributor to bone weakness. These findings add new knowledge to how *in utero* alcohol exposure affects the offspring.

ACKNOWLEDGEMENTS

All praises are due to Allah for sparing my life to this very day and making this research a successful one. Firstly, I would like to express my sincere appreciation to my supervisors: Dr. Robert Ndou and Mrs. Diana Pillay, who introduced me to this interesting topic and to the field of scientific research in general and supplied me with adequate materials. Their offices were always open for me to receive words of encouragement, guide and all forms of support throughout the period of the research work. I cannot thank you enough and you forever remained my mentors.

I am grateful to the entire staffs of the School of Anatomical Sciences, University of the Witwatersrand for helping me either directly or indirectly. Special appreciation goes to Mrs. H. Ali for the technical support she provided throughout the research period. Her encouraging words will continue to linger in my mind.

I am much grateful to the staff of the central animal service, for assisting with animal care and carrying out procedures.

My sincere appreciation goes to Kudawashe Jakata for his persistent and tireless efforts in helping with the micro-focus x-ray computed tomography imaging of the bones tissues.

I remain grateful to my numerous friends and family that helped with prayers and support, either directly or indirectly. Your names are too many to be mentioned. My special regards to entire family of Alhaji Ibrahim Bala (Baba Ibrahim) for the kind support given to my wife and children (Zainab and Nafeesa) while I was away. Thanks to my lovely wife (Aisha Umar) for being strong and supportive. You would forever remain cherished by me.

My appreciation goes to National Research Foundation (NRF) for funding the research work and the management of Federal University Birnin Kebbi, Kebbi State, Nigeria for the sponsorship.

TABLE OF CONTENTS

LIST OF ABBREVIATIONS

%:	Percent
^{o}C:	Degree Celsius
β:	Beta
µm:	micrometer
dl:	deciliter
kg:	kilogram
ml:	milliliter
mg:	milligram
mm:	millimeter
nm:	nanometer
µCT:	Microfocus x-ray computed tomography
AESC:	Animal Ethics Screening Committee
ANOVA:	Analysis of variance
APES:	3-aminopropyltriexothysilane
ARBD:	Alcohol-related birth defects
ARND:	Alcohol related neurodevelopmental disorder
BT/TV	Bone to total volume
CAS:	Central animal services
CDC:	Center for disease control and prevention
CDK	Cyclin dependent Kinase

CNS:	Central nervous system
CRL:	Crown-Rumph length
DAB:	3-3’ di-amino benzidine
DNA:	Deoxyribose nucleic acid
EDC:	Ethanol-derive calories
EDTA:	Ethylenedeamine tetraacetic acid
FAS:	Fetal alcohol syndrome
FASD:	Fetal alcohol spectrum disorder
FIG:	Figure
H_2O_2:	Hydrogen peroxide
H&E:	Haematoxylin and eosin
Ica:	ionized calcium
IHC:	Immunohistochemistry
IOM:	Institute of medicine
IUFD:	Intrauterine fetal death
OFC:	Occipitofrontal circumference
PBS:	Phosphate buffer solution
pDXA:	Peripheral Dual-energy x-ray absorptiometry
PFAS:	Partial fetal alcohol syndrome
pH:	Potential of hydrogen
PTH:	Parathyroid hormone
SD:	Standard deviation

SES:	Socioeconomic status
TbN	Trabecular number
TbSp:	Trabecular separation
TbTh:	Trabecular thickness

LIST OF FIGURES

LIST OF TABLES

STRUCTURE OF THE DISSERTATION

The dissertation was written in four chapters. In the first chapter, a general introduction on FAS were provided. Moreover, the aims and objectives of the study, justifications as well as the hypothesis were explained. The chapter also covered the literature review of the related topic, rate of alcohol consumption among pregnant women as well as prevalence and features of FAS. It also covered bone development and the mechanisms by which intrauterine alcohol exposure affects bone development.

The second chapter explained the materials and methodology applied in the study. It explained in details the procedures and protocols involved in immunohistochemistry and the three-dimensional micro-focus x-ray computed tomography investigations.

The result of the study were presented in chapter three, while the discussion, conclusion, limitations of the study as well as recommendations were presented in chapter four.

1 GENERAL INTRODUCTION

Alcohol is a teratogenic agent and is the second most widely used psychoactive substance worldwide (Zakhari and Li, 2007). Despite an awareness of the deleterious effects of alcohol consumption, acute and chronic alcoholism is increasing among old and young populations including pregnant women (Chen et al., 2001). The rate at which pregnant women of child bearing age consume alcohol is increasing (20%), worldwide (Chang et al., 2000). Alcohol consumption at this stage can result in a variety of disorders to the developing fetus, collectively referred to as fetal alcohol spectrum disorders (FASD). These may include fetal alcohol syndrome (FAS), which is the most severe and extreme end of the spectrum of these disorders. It (FAS) is the commonest cause of growth retardation in the Western world (Medina, 2011). It is also associated with persistent physical and neurodevelopmental abnormalities across all socioeconomic groups, races and ethnicities. The incidence of FAS is increasing, making alcohol use during pregnancy an important public health concern among women and their unborn children (Ramadoss et al., 2006).

Fetal alcohol syndrome is characterised by growth and mental retardation, facial dysmorphogenesis and neurodevelopmental abnormalities (Ernhart et al., 1985; O`Leary, 2004; Simpson et al., 2005; Carvalho et al., 2016). Although it is difficult to diagnose at early age growth retardation remains the cardinal feature of FAS (Day, 1992; Ramadoss et al., 2006).

Several studies investigating the effects of gestational alcohol on the prenatal development of the osseous tissue to understand the resultant growth retardation exist in the literature (Miralles-Flores and Delgado-Baeza, 1992; Keiver et al., 1997). In contrast, studies on these in utero alcohol effects in postnatal development of the osseous tissue are limited (Miralles-Flores and Delgado-Baeza, 1992; Nwaogu, 2002). The mechanisms involved in the observed growth retardation following gestational alcohol exposure are still unclear, which warrants further investigations.

1.2 AIMS AND OBJECTIVES

1.2.1 Aims

This study aims to determine the effects of prenatal alcohol exposure on the distal growth plate of postnatal three-week-old *Sprague-Dawley* rat tibia.

1.2.2 Objectives of the present study

1. To test whether gestational alcohol exposure affects the tibial growth plate.
2. To investigate whether gestational alcohol exposure affects cellular proliferation in the tibial growth.
3. To investigate whether gestational alcohol exposure affects internal tibial bone morphology.

The result of this study could go a long way in adding knowledge to the field of research as well as a tool for further research. It could also add clinical information on how prenatal alcohol exposure can lead to osteoporosis with subsequent pathological fracture.

1.3 LITERATURE REVIEW

1.3.1 Fetal alcohol syndrome (FAS)

Maternal alcohol ingestion adversely affects the developing fetus in various ways such as spontaneous abortion, intrauterine fetal death, asphyxia, low birth weight, and perinatal mortality (Carvalho et al., 2016). A spectrum of disorders which include: fetal alcohol syndrome, partial fetal alcohol syndrome, alcohol related neurodevelopmental disorder, and alcohol-related birth defects. Also associated with these adverse effects are collectively referred to as fetal alcohol spectrum disorder, with fetal alcohol syndrome being the most severe form of the disorder (Ethen et al., 2009).

Lemoine (2003) first described the pattern of disabilities associated with prenatal alcohol exposure in France in 1968. The name, Fetal alcohol syndrome was first documented in 1973 by Jones and Smith in United States (Urban et al., 2008). This condition is characterised by a pattern of pre and postnatal growth retardation, facial dysmorphology and central nervous system deficits. These features can appear in milder forms in some exposed children who may not be diagnosed with fetal alcohol syndrome. Therefore, the consequences of prenatal alcohol exposure ranges from mild effects to full blown features of fetal alcohol syndrome (Larkby and Day, 1997). The subtle nature and lack of accurate knowledge of associated features in neonates and infants makes diagnosis of fetal alcohol syndrome difficult and often missed during these early life periods. Due to the complexity and range of dysfunctions linked to prenatal alcohol exposure, a multidisciplinary approach is required to achieve accurate diagnosis and treatment recommendations (Chudley et al., 2005).

Alcohol consumption in pregnancy

Manifestation of full blown features of FAS is dependent on the timing, dosing and maternal drinking pattern. Research shows an increase in alcohol use among pregnant women worldwide (Olegård et al., 1979; Larkby and Day, 1997; Croxford and Viljoen, 1999; Ornoy and Ergaz, 2010). In the United States of America, the center for disease control and prevention (CDC) reported a rate increase from 12.4% in 1991 to 16.3% in 1995. In South Africa, a study in rural and urban areas of the Western Cape Province shows that 42.8% of the women admitted to varying degrees of alcohol consumption during pregnancy. Some (23.7%) were regarded as significant drinkers (moderate or heavy alcohol drinking in a binge pattern) (Croxford and Viljoen, 1999).

The term pregnancy risk-drinking is defined as the consumption of one ounce or more of alcohol (two or more drinks) per day (Chang, 2001). The following general definitions of drinking pattern is therefore used to identify harmful effects of alcohol consumption:

(i) binge drinking (≥4 drinks per occasion for women and ≥5 drinks per occasion for men),

(ii) heavy drinking (>1 drink per day on average for women, and >2 drinks per day on average for men),

(iii) any alcohol consumption by youth aged < 21 years, and any alcohol consumption by pregnant women.

These definitions are consistent with what is obtainable from CDC and the National Institute on Alcohol Abuse and Alcoholism (Bouchery et al., 2011).

While heavy drinking in pregnancy is known for its adverse effects on the offspring, small amounts of alcohol intake (0.5 drinks per day) may also have adverse effects (Sokol et al., 1980). This was observed in a study at Yale-New Haven Hospital that reported an association between intrauterine growth retardation (birth weight less than the 10th percentile for each gestational week) and mild alcohol ingestion (>0.10 to 0.25 ounce) during pregnancy (Lundsberg et al., 1997). These studies indicate that there is no universally accepted safe amount of alcohol use during pregnancy. However, the severity of these effects tends to be proportional to the amount of alcohol consumed (Windham et al., 1995).

Features of FAS and diagnostic criteria

In recent years, diagnosis of FAS has undergone a series of modification since its ealier description by Jones and colleagues in 1973. The main challenge is that there is no standard laboratory tests for the diagnosis of FAS. As a result, different diagnostic criteria are used in delineating the features of FAS (May et al., 2014).

Although these criteria differ in mode of diagnosis, they share similar definitions of FAS features. These are: pre or postnatal growth retardation, facial abnormalities (short palpebral fissure, indistinct philtrum, short nose, epicanthic folds, depressed nasal bridge, thin vermillion, and micrognathia) and central nervous system abnormalties (mental retardation, behavioural problems, poor concentration and attention, social withdrawal and conduct problems) (Riley et al., 2011). These features have been defined by four different diagnostic criteria which include: 4-digits code, revised-institute of

medicine (IOM), Canadian guidelines for diagnosis, national task force/CDC guidelines (Table 1.1) (Riley et al., 2011). However, diagnosis require a history of maternal alcohol ingestion (O'Leary, 2004).

1.3.2 Prevalence of FAS

Varying research methods

Studies determining the prevalence of FAS encountered several challenges such as, case finding, sampling, diagnostic criteria, variation in methodology, and coordination of interdisciplinary activities (May et al., 2009). Moreover, surveillance systems: prenatal clinic-based studies and special referral clinics have been proven to be inadequate in determining the prevalence of FAS. The inadequacy may be associated with a lack of standard diagnostic criteria, and denial of history of maternal alcohol ingestion (May et al., 2014).

Due to these challenges, estimating the prevalence of FAS varies from one country to another and between geographical and cultural settings of communities within the same country (May and Gossage, 2001). These considerable variations among different countries make reliably estimating the global prevalence of FAS difficult (Roozen et al., 2016).

Table 1.1: **Summary of various diagnostic criteria of FAS and definition of clinical features.**

Features of FAS	4-digits code	Revised IOM	Canadian guidelines	National task force/CDC
Growth retardation	Height and weight below the 10th percentile for age.	Height and weight below the 10th percentile for age.	Height and weight below the 10th percentile for age or low weight to heigth ratio.	Height and weight less than the 10th percentile at any point in time.
Facial abnormalities	Presence of the following: short palpebral fissure, thin vermillion border and indistinct philtrum.	Presence of two or more of the following features**:** short palpebral fissure, thin vermillion border and indistinct philtrum.	Presence of the following: short palpebral fissure, thin vermillion border and indistinct philtrum.	Presence of the following: short palpebral fissure, thin vermillion border and indistinct philtrum.
CNS anomalies	Occipitofrontal circumfrence (OFC) below normal (≤2 SD) or significant brain abnormalites or function.	OFC less than the 10th percentile or presence of structural brain abnormality.	CNS impairment: brain sructure; cognition; communication; academic performance; memory; abstract	OFC below the 10th percentile or structural brain abnormality.

Various epidemiological methods are used worldwide to delineate the prevalence of FAS. The three main methods are: passive method (use of birth certificates and special registry); clinical based studies (screening of pregnant women for alcohol abuse and follow-up) and active case ascertainment method (targets referrals of all children with FAS) (Warren et al., 2001). Of these methods, the passive method, which relies on pre-

existing health records is less expensive and less time consuming. However, this method is associated with lack of general consistency due to its overdependence on the quality and completeness of the existing births and special registries, as well as diagnostic efforts of non-specialist and other health care providers (May et al., 2009).

In contrast, the active case ascertainment method provides active, effective and comprehensive focus on a specific population at a particular geographical location (May and Gossage, 2001). Compared to other methods, the active case ascertainment method provides the best coverage of FAS. This method also allows active recruitment and case finding of children with FAS (May et al., 2009).

Prevalence of FAS in developed countries

In the United States, the CDC's Birth Defects Monitoring Program reported a prevalence of 0.2 per 1000 live births from 1979 to 1992. A higher rate of 0.3 and 0.67 per 1000 live births was reported between 1992 and 1993. The rate varies between ethnic groups from 1981 to 1986 as follows: 0.6 per 1000 live births among African-Americans, 0.08 among Hispanics, 2.9 among American-Indians, 0.03 among Asians, and 0.09 among whites (May et al., 2009). A relatively recent study conducted using the active case ascertainment method in a Midwestern community among first grade students (6 to 7 years old) reported a rate of 6 to 9 per 1000 children (May et al., 2014). Generally, the most widely accepted prevalence is 0.97 per 1000. This is the representation of the combined averages from various prospective studies in the country (Warren et al., 2001).

In Australia, a comprehensive estimate was obtained from a combined data from the Western Australia Birth Defects and Rural Pediatric Services. The findings reported a prevalence of 0.02 per 1000 live births for the non-Aboriginal children, and 2.76 per 1000 live births for the Aboriginal children. In the Northern Territory, data obtained from retrospective study of medical records and outpatient correspondence of children born from 1999 to 2000 showed a prevalence of 0.68 per 1000 live births. Likewise, an average rate of between 1.87 and 4.7 per 1000 live births for indigenous children was found (May and Gossage, 2001).

In Canada, there is no standard national statistics on the prevalence of FAS. However, different studies estimated the rate from different communities of British Columbia, Manitoba, and Saskatchewan. In British Columbia and Manitoba, the prevalence is 190 per 1000 and 55 to 101 per 1000 live births respectively. Based on referral to the diagnostic centers, the rate was estimated to be 0.589 per 1000 live births in Saskatchewan (Chudley et al., 2005).

Prevalence of FAS in South Africa

There is no standard national surveillance system to determine the nationwide prevalence of FAS in South Africa. However research has been conducted in this area, and different researchers have documented a high prevalence of FAS from various communities in different provinces of the country (Viljoen et al., 2005; May et al., 2013; Olivier et al., 2016). Three consecutive case ascertainment methods indicate a high prevalence among first graders in a Western Cape community (Table 1.2).

Table 1.2: Prevalence findings of FAS among different communities in South Africa.

Study	Setting	Socioeconomic status (SES)	FAS cases per 1000
Active case ascertainment (May et al., 2009)	Western Cape	Coloured population (low and middle SES) White population (middle and upper SES)	40.5 – 46.4
Active case ascertainment (Viljoen et al., 2005)	Western Cape	Coloured population (low and middle SES) White population (middle and upper SES)	65.4 – 74.2
Active case ascertainment (May et al., 2007)	Western Cape	Coloured population (low and middle SES) White population (middle and upper SES)	68.0 – 89.2
Active case ascertainment (Urban et al., 2008)	De Aar (Northern Cape)	Coloured/black (low and middle SES)	111.4
	Upington (Northern Cape)	Coloured/black (low and middle SES)	74.7
Active case ascertainment (Rosenthal et al., 2005)	Gauteng	Blacks (middle and low SES)	20

Although Cape Town is the most densely populated and major city in the Western Cape, about 40% of the population lives in the outer smaller towns and rural areas. The estimated population of the province is 3,721,200. Fifty-seven percent (57%) of the population are of mixed race (coloured), 18% black, 25% white and 1% other races (Viljoen et al., 2005). Alcohol use is highest in the province even among pregnant women, with over 20% of pregnant women drinking in a binge pattern (Viljoen et al., 2005). The high rate of alcohol use and FAS was found to be associated with some specific risk

factors. These include poor socioeconomic status, poor maternal education, genetic and environmental factors (Urban et al., 2008).

The Western Cape is a grape and wine producing area, contributing to the drinking pattern of its inhabitants. The dop system could be traced back to the colonial era in 17th century and has contributed siginificantly to high rate of alcohol use especially in the western cape. As such, the province has the highest prevalence of FAS in the world. It is a condition in which farm workers were provided with food or wine as part of their wages. Although is presently outlawed by different legislative bodies, minotrity of the farms are currently and actively practising the system (Viljoen et al., 2005).

1.3.3 Growth retardation resulting from prenatal alcohol exposure

Prenatal alcohol exposure results in growth deficiency, low body weight, short stature, and low weight to height ratio (O'Leary, 2004). Even in adulthood, osteoporosis and fractures are common among individuals that were exposed to alcohol prenatally. Research suggests that these effects may not be reversible despite adequate nutrition (Simpson et al., 2005).

Rodent models of FAS show features such as low body weight, shorter bone length, delayed fetal skeletal ossification, and low skeletal maturity scores (Keiver et al., 1997; Keiver and Weinberg, 2004). These characteristics persist till weaning (3-week-old pups), however, possible effects at later stages have not been studied. Intrauterine alcohol exposure has also been shown to affect functional measures in bone health as seen in the study by Given and colleagues (2004), who reported that bone strength was altered

by maternal ethanol intake in fetal sheep. Studies suggest that low birth weight and impaired bone growth as well as a decrease in mineralisation *in utero* may reduce peak bone mass which increase the risk of osteoporosis later in life (Jones and Dwyer, 2000; Cooper et al., 2001; Godfrey et al., 2001).

1.4 BONE DEVELOPMENT

To investigate how prenatal alcohol exposure affects the skeletal system, it in crucial to undertand how bone develops. Bone development comprises a series of complex processes which include cellular positioning and matrix deposition. This process of new bone formation is dependent on the biochemical environment. It is possible that prenatal elchohol exposre may alter the biochemical environment resulting in small, weaker bones at birth. Bone development (ossification) occurs by two distinct mechanisms: intramembranous bone ossification and endochondral bone ossification (Shapiro, 2008).

1.4.1 Intramembranous bone ossification

Intramembranous ossification is responsible for the formation of most of the craniofacial bones and the clavicle (Ortega et al., 2004). It occurs by initial rapid proliferation and differentiation of neural crest-derived mesenchymal cells to osteoblasts. This is then followed by mineralisation of the collagenous framework produced by the differentiating osteoblasts (Percival and Richtsmeier, 2013).

1.4.2 Endochondral bone ossification

Endochondral ossification is responsible for the formation of most of the vertebrate appendicular and axial skeleton. In this process, the mesenchymal cells differentiate into a cartilage model. This occurs at two different sites in developing long bone: the primary (diaphyseal) and secondary (epiphyseal) sites of ossification (Ortega et al., 2004).

Primary ossification

Primary ossification involves the initial appearance of a cartilage model formed by condensation of mesenchymal cells (Fig. 1.1). Later, the cartilage is differentiated into chondrocytes that secrete extracellular matrix components. The cartilage model serves as a template for longitudinal growth in long bone formation. Once formed, the cartilage is invaded by differentiated osteoblasts at the center, forming a collar-shape primary center of ossification (Mackie et al., 2008).

The cartilage enlarges in width and length, and is then subsequently invaded by new blood vessels (neovascularisation) within the primary bone collar leading to a transient stage of endochondral bone formation in the medullary canal and endosteal surface. Further growth of the diaphysis is achieved by direct appositional growth and restoration in the periosteal and endosteal surfaces respectively (Carter et al., 1996). Chondrocyte differentiation and neovascularisation are essential for smooth progression of endochondral ossification, this maintains normal fetal growth, as well as bone remodelling and repair in adult life (Stevens and Williams, 1999).

Fully matured and differentiated osteoblasts are responsible for collagen (mainly type I) and alkaline phosphatase secretion. These are essential for extracellular matrix deposition and maturation. Moreover, non callagenous proteins (osteocalcin, osteopontin, osteonectin) are secreted by the osteoblasts. These proteins regulate maturation of the extracellular matrix. At the end of their lifespan, osteoblasts are found either lining the bone surface or trapped within the matured matrix, referred to as osteocytes (Eriksen, 2010).

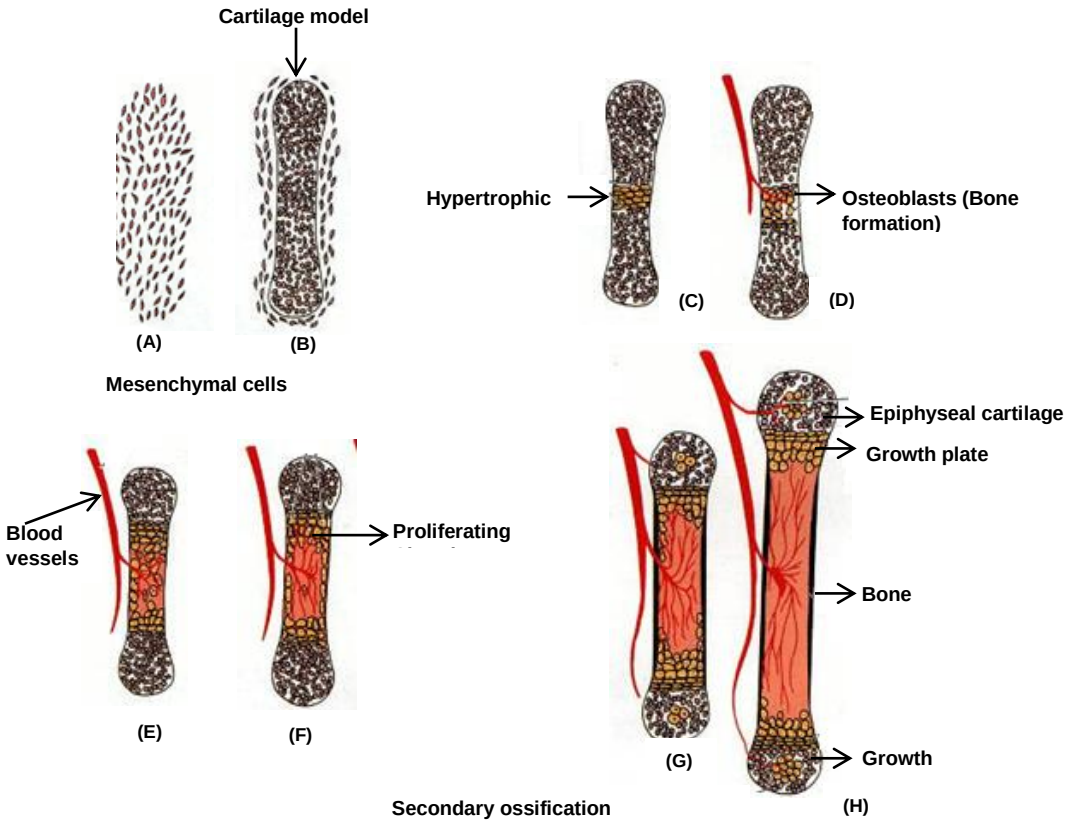

Figure 1.1: Schematic representation of endochondral ossification. (A, B) Condensation of mesenchymal cells, differentiate into chondrocytes which produces the cartilaginous model of the bone. (C) Chondrocytes in the center of diaphysis undergo hypertrophy and apoptosis while they change and mineralise their extracellular matrix. Apoptosis of chondrocytes permits blood vessels to enter. (D, E) Blood vessels carry in osteoblasts, these bind to the degenerating cartilaginous matrix and deposit bone matrix. (F-H) Bone development and growth consist of proliferating, hypertrophic, and mineralising chondrocytes. Secondary ossification centers also form as blood vessels enter near the epiphysis of the bone. (Image adapted from Gilbert SF, 2000).

Secondary ossification

In long bones, the epiphysis and metaphysis originate from an independent secondary ossification center. These two parts are separated from the diaphysis by segregation of differentiating chondrocytes collectively referred to as the growth plate. The growth

plate is the main source of longitudinal growth in the developing long bone (Stevens and Williams, 1999). Irrespective of stage of development, the chondrocyte segregations (zones) and morphology are distinct (Fig. 1.2). Their distinction reflects changes in functional stages of the cells (reserve, proliferative and hypertrophic zones) (Mackie et al., 2008).

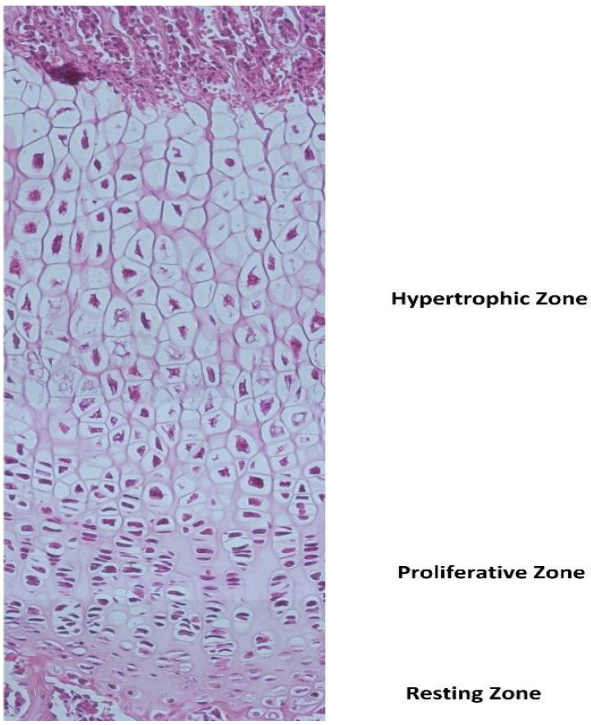

Figure 1.2: Photomicrograph showing different chondrocytes morphology in different zones of the epphyseal growth plate (Image courtesy of Bello NK and Perry V).

Reserve cell zone

The layer furthest away from the ossification front is called the reserve cell zone. It is sometimes referred to as stem, germinal or resting cells zone (Fig 1.2). It is narrow,

consisting of single and paired irregularly arranged chondrocytes (Hunziker, 1994). In this zone, more of the extracellular matrix is deposited and the cells are dispersed and relatively quiescent (Ballock and O'keefe, 2003). The cells have many short filopodia extending from the plasmalemma to the surrounding matrix, giving them a scalloped appearance (Howlett, 1979). The reserve cell zone corresponds to the preparatory phase of rapid chondrocytes division, thereby contribituing to the longitudinal bone growth (Hunziker, 1994).

At an early stage of development, the adjacent zone still consists of an epiphyseal plate called the reserve zone cartilage. At maturity, the zone becomes embedded into the epiphyseal bone tissue (Hunziker, 1994).

Proliferative zone

The proliferating zone lies adjacent to the resting zone and the cells undergo rapid division (Fig 1.2). These cells appear granular coated which is believed to be from the product of the cells and discoid when viewed transversely. The cellular arrangement towards the pre-hypertrophic zone are disorganised and separated by a large amount of matrix (Howlett, 1979). This zone is crucial as it is possible that alcohol may impair cell division here and result in stunted growth.

Hypertrophic zone

In the hypertrophic zone, cellular division ceases and the cells begin to increase in size and are terminally differentiated (Fig 1.2). The size attained during hypertrophy is largely determined by the rate of proliferation. This terminal differentiation is associated with a

marked increase in alkaline phosphatase acitvity, synthesis and secretion of type-X collagen (Lui et al., 2011). The cells appear to have numerous matrix vesicles formed by budd6ing on the plasma membrane (Ballock and O'keefe, 2003). The cells eventually undergo apoptosis and of the transverse septa of cartilage matrix surrounding the cells break down. The vertical septa remain largely intact thereby allowing entry of the invading cells of ossification: osteoblasts precursor; osteoclasts; bone marrow cells as well as blood vessels (Ortega et al., 2004).

1.4.3 Maintenance of bone structure

Bone structrue and function is maintained during adulthood by the processes of remodelling and consolidation. Bone remodelling is a process of bone renewal to maintain its normal strength and homeostasis. Old and dead parts of the bone are replaced with newly synthesised and mineralised matrix (Clarke, 2008). The process follows sequential and regulated phases of resorption and formation that take place in what is termed Basic Multicellular Unit, which comprises osteoblasts, osteoclasts and osteocytes (Eriksen, 2010).

The process of bone resorption is initiated by osteoclasts, which erode dead bone causing a lacuna called a resorption lacuna. The depth of the lacuna varies from 60µm in young adult to 40µm in the elderly. This is then followed by new bone formation by the osteoblasts (Eriksen, 2010).

1.5 BONE STRUCTURE AND FUNCTIONS

In order to investigate the effects of gestational alcohol on the skeletal system, it is vital to undestand its structure and funcion. Bone is a specialised and complex tissue that performs two basic functions: mechanical and metabolic functions. Metabolically, bone is the major store or resevoir of calcium and phosphate (Weiner and Wagner, 1998). Mecha6nically, bone acts to protect the internal organs, load bearing, allows locomotion and houses the marrow stroma responsible for hematopoiesis (production of blood cells) (Boskey and Coleman, 2010).

Four bone types exist; long, short, flat, and irregular bones. It is known that prenatal alcohol exposure results in stunted growth (Nwaogu, 2002; Simpson and Keiver, 2005; Snow and Keiver, 2007). Considering that long bones are important for height and growth, this study will pay attention to long bones.

A long bone is composed of the diaphysis (shaft), epiphysis (larger upper and lower ends), and metaphyisis (an area between the diaphysis and epiphysis), which contains the growing cartilage (Fig. 1.3). Structurally, bone can be further classified into cortical (compact) and trabecular (cancellous) bone. The structures are better differentiated using histological evaluation (Rho et al., 1998).

1.5.1 Cortical bone

Cortical bone is a dense layer forming the outer wall of the diaphysis of long bone. It accounts for about 80% of the bone mass (Wehrli, 2007). The external surface of compact bone is covered by periosteum acting as a transition layer between the bone

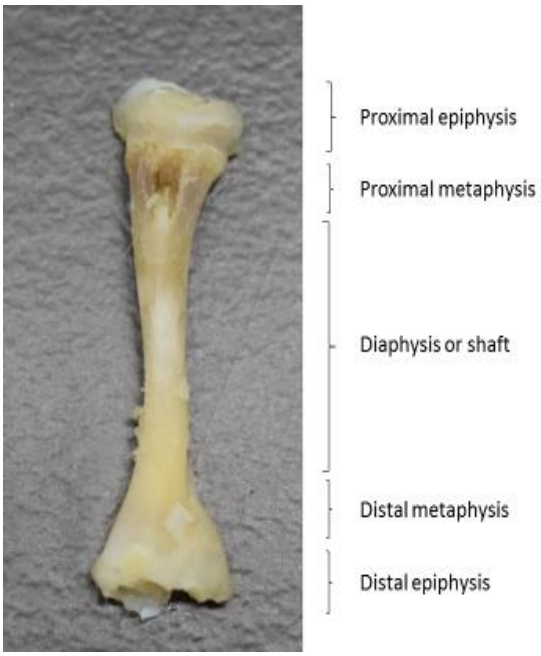

Figure 1.3: General architecture of a long bone (Right tibia). The metaphysis is an area between the diaphysis and epiphysis (Image courtesy of Bello NK and Perry V).

and overlying tissues. Histologically the periosteum comprises of two layers: the outer fibrous layer and the inner cambium layer. The fibrous layer is composed of the superficial and the deep layer. The superficial layer is predominantly collagenous with few elastic fibers and is highly vascularised, contributing significant blood supply to the bone. The deeper layer is fibroelastic, less vascularised and recieves most of tendinous insertions (Dwek, 2010).

The inner cambium layer lies in direct contact with the bony surface. It is highly cellular and comprises of adult mesenchymal progenator cells, fibroblasts and osteoblasts. These cells are important in periosteal bone formation and are a source of osteoprogenator cells (Allen et al., 2004).

Collagen fibrills, mainly type 1 collagen are the building blocks of compact bone. These collagen fibrils are secreted and arranged in an extracellular matrix interspersed by mineral crystals of calcium hydroxyapatite and water (Viguet-Carrin et al., 2006). They are arranged in a planner pattern called lamellae of 3 to 7µm wide (Fig. 1.4). They may also be arranged in a concentric layer surrounding a central canal, forming what is known as the osteon or Harvesian system. The osteon is about 200 to 500µm wide, running parallel to the long axis of bone (Rho et al., 1998) and connected together at a right angle by a canal called Volkmann's canal. The Volkmann's canal is lined internally by multiple layers of metabolically active osteoblasts and osteocytes during bone remodelling (Wehrli, 2007).

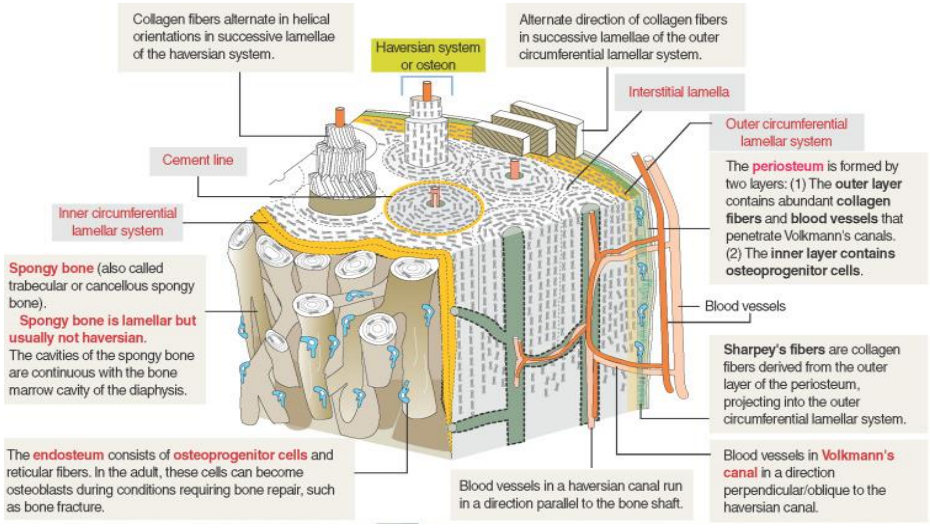

Figure 1.4: Microarchitecural structure of compact bone showing the haversian system. Some parts of the outer layer of the periosteum enters the Volkmann's cannal giving the thick anchoring collagen fibers called the Sharpy's fibers (Image adapted from Keirszanbaum and Tres, 2012).

1.5.2 Trabecular bone

Trabecular or cancellous bone is distributed within the medullary space of the cortical bone and epiphyseal end of long bone in higher quantity (Gibson, 1985). It is a network of cellular structures shaped into rods and plates. The rods and plates give the cells a characteristic open and closed shaped structures respectively (Fig 1.5). The cells in plate-like parts are not completely closed, thereby allowing communication with the marrow stroma (Gibson, 1985). The rods and plates are attached in a three-dimensional arrangement. This connectivity is essential in maintaining sufficient tensile strength of bone (Dempster, 2000), and largely dependent on the connections of trabecular plates to struts (Hahn et al., 1992).

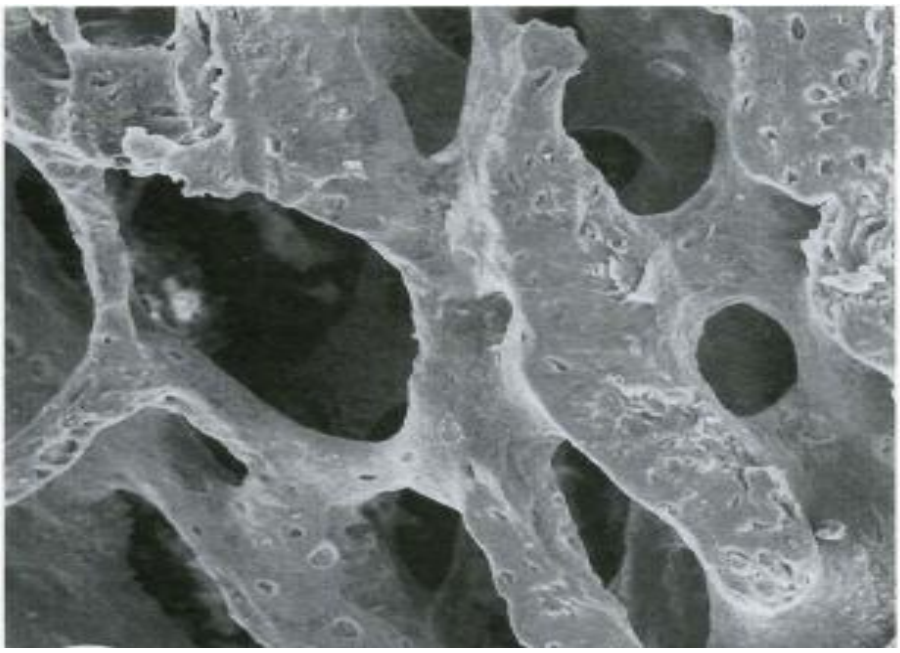

Figure 1.5: Trabecular bone structure of the distal metaphysis of the hamster femur. The trabecular appears thick and continous (Chen et al., 2001).

In human bone (iliac crest), specifically, the trabecular thickness ranges between 100 to 500μm thick, and is lined internally by a layer of endosteal cells called osteoblasts with occasional multinucleatetd osteoclasts lining its margin. Externally, the whole structure is completely enclosed by a thin cortex making the bone spongy and lighter. The trabecular structure and its vasculature provides a larger surface area and vast substrate for cellular interaction. It also provides the basic frame work, nutritional supply and waste removal for effective haemopoiesis (Wilkins, 1992).

1.6 EFFECTS OF ALCOHOL ON BONE DEVELOPMENT

1.6.1 Direct effects of alcohol on osteoblasts and on the growth plate

Osteoblhasts are the principal cells in bone formation, and are directly affected by alcohol during bone formation. For example, in an *in vitro* environment, using human osteoblasts, alcohol caused a reduction in proliferation and osteoblasts number (Chavassieux et al., 1993). This reduction in osteoblasts number occured in a dose dependant manner (Friday and Howard, 1991), and may be as a result of overt toxicity or inhibition of intracellular cell proliferation signalling processes such as a reduction in polyamine levels. Polyamines (putriscine, spermidine, and spermine) are aliphatic amines that are implicated in cellular proliferation and division. It is possible that alcohol may affect their expression and function (Heby, 1981).

Osteocalcin is expressed by osteoblasts and is thought to serve as a marker for osteoblastic function. Serum osteocalcin level in human alcoholics has been found to be low, suggesting a secondary decrease in osteoblastic number and activity (Labib et al., 1989). Lower serum osteocalcin level was also reported in alcohol exposed rats when compared to those on isocaloric controlled liquid diet. This was proposed to be as a result of alcohol effects on osteoblasts proliferation and activity (Peng et al., 1991).

Apart from alcohol effects on the osteoblasts, alcohol can also directly affect morphology of the growth plate during early and late developmental stages. These changes involve a reduction in length of resting and hypertrophic zones as well as a shorter diaphysis. This leads to the subsequent reduction in fetal bone length. These effects on the resting and

hypertrophic zones suggests early and late damage of fetal bone development respectively (Snow and Keiver, 2007).

Alcohol has adverse effects on the bone marrow, causing alteration in osteogenic differentiation, thereby promoting an increase in bone marrow fat content. This is suggestive of alcohol induced reduction in osteoblastic number and activity with subsequent reduction in bone formation (Gong and Wezeman, 2004). Another *in vitro* investigation showed that alcohol shifts the lineage committement of mesenchymal stem cells towards adipogenesis. This reults in deposition of more adipose tissue in the bone marrow stroma and subsequent osteopenia (reduction in bone mineral density) (Wezeman and Gong, 2004).

1.6.2 Indirect effects of alcohol on growth and development

Alcohol impairs calcium metabolism and homeostasis, indirectly affecting the role of calcium on bone growth and development. Calcium is an abundant nutrient in the body. Over 99% is stored in bone, while only 1% is found in the circulation in an ionised form (Ca^{2+}). It is a crucial nutrient in bone formation, bone strength, and reduces osteoporosis fracture risk (Beto, 2015). Calcium homeostasis is also essential in maintaininag normal fetal growth and development. A study reported decreased fetal calcium levels as well as a decrease in physiological pH of fetal rats prenatally exposed to alcohol. Consequently, there was a reduction in fetal bone ossification with secondary reduction in fetal body weight and length (Keiver and Weinberg, 2004). In a similar study, a reduction in bone formation was observed in fetuses prenatally exposed to alcohol. This

reduction occurred through low calcium, calcium-regulating hormones and osteocalcinin fetal circulation (Keiver et al., 1996).

Vitamin D, parathyroid hormone (PTH), and calcitonin, are crucial hormones in regulating and maintaining Ca^{2+} level in the circulation. In cases of low Ca^{2+} level, PTH stimulutes the productuon of Vitamin D and acts synergistically to cause bone resorption and subsequently increses Ca^{2+} in the circulation. Parathyroid hormone also decreses the rate of calcium loss via the urine (Keiver et al., 1996).

1.7 CELL DIVISION

Cell division refers to a process by which cells produce two symmetrical or asymmetrical daughter cells (Roach et al., 1995). The latter, refers to the two daughter cells having a distinct fate due to differences in shapes, sizes, morphological or biochemical features (Horvitz and Herskowitz, 1992). Different cell type such as growth plate chondrocytes have been used to study the mechanisms of asymmetrical division (Jan and Jan, 1998).

A study using male Long-Evans rats showed how chondrocytes in the proliferating zone of growth plate passes through different phases of division. The phases occur at a different rate over a single period of time (Wilsman et al., 1996), and in a regulated fashion called cell the cycle (Elledge, 1996). Generally, the cell cycle is composed of four stages of development: the gap before deoxyribonucleic acid (DNA) replication (G_1), the phase of DNA synthesis or replication (S), the gap after DNA replication (G_2), and the mitotic phase (M) during which cell division occurs (Table 1.3) (Hartwell and Weinert, 1989). It is not clear whether gestational exposure affects or delays these phases of cell division.

The mitotic stage comprises of four principal phases: prophase, metaphase, anaphase, and telophase. In prophase, chromosomal condensation and spindle is formed (King et al., 1994), this is followed by migration and alignment of the chromosomes to the opposite end (equatorial plane) of the cell in metaphase (Winey et al., 1995).

In anaphase, two identical daughter chromosomes are produced from the cleavage of cohesion that binds the sister chromatid together. This is then followed by the final

stage, telophase, which is characterised by chromosomal uncoiling, development of two separate nuclei, and ultimate division of the cytoplasm to two daughter cells (FitzHarris, 2012).

Table 1.3: Phases of cell cycle

State	Phase	Description
Resting	G_0	The cell exit the cycle before commitment to DNA replication in subsequent cycle. It is a non-growing and non-replicating phase (Nurse, 1994).
	G_1	The cell in this stage prepare for DNA replication by increasing in size with intact control mechanism (check point) to ensure subsequent and effective DNA replication (Nurse, 1994).
Interphase		
	S	Phase of DNA replication (Nurse, 1994).
	G_2	The cell continue to grow and prepare for the next mitotic stage (Schafer, 1998).
Mitosis	M	Mitotic phase comprises of steps or pathways within the cell responsible for cell duplication and division (King et al., 1994).

The cell cycle is controlled by complexes cyclin-dependent kinase (CDK) and cyclin (regulatory subunit). The two complexes are further regulated by three dependent mechanisms: abundant cyclin subunit, phosphorylation status of the CDK, and the presence of inhibitory proteins, cyclin dependent kinase inhibitors (LuValle and Beier,

2000). It is not clear whether alcohol acts in one of these stages and future research may shed light on these questions.

2 MATERIALS AND METHODS

2.1 INTRODUCTION

Animal studies are the basis of understanding the underlying mechanisms of alcohol's teratogenicity. Human studies in this area are limited since pregnant women who drink alcohol may not volunteer for studies. Also, ethical considerations make it hard to use humans. For example, administration of alcohol to pregnant women is prohibited. Consequently, animal models are necessary to investigate the effects of gestational alcohol exposure on the developing embryo.

The existing animal models include: rats, mice, guinea pigs, sheep, chick, zebrafish and non-human primates (Pattern et al., 2014). Due to their cost effectiveness, short gestation, ease of handling, high fertility and large litter size, rats are the most widely used animals in FAS research. Rats follow the same pattern of bone growth and development (endochondral ossification and periosteal bone formation) as humans. They also undergo the same age related bone loss as humans. However, it is crucial to acknowledge that rats are born at a stage of development that is prematurely relative to humans. With regards to osseous tissue development, a term rat is approximately equivalent to an early second trimester human fetus (Pattern et al., 2014). The development of long bones which is responsible for longitudinal growth occurs during the first trimester (Snow and Keiver, 2007).

2.2 STUDY SETTING

2.2.1 Study animals

The study was approved by the Animal Ethics Screening Committee (AESC), University of the Witwatersrand, Johannesburg (AESC 2015/27/15C) prior to commencement. Fifteen (15), three-months-old, virgin female *Sprague-Dawley* rats weighing an average of 300g were used. All the animals were sourced and housed at the Central Animal Services (CAS), University of the Witwatersrand. The animals were housed in transparent plastic cages lined with wood dust, with unlimited access to food and water. Room temperature was maintained at 23±2^{o}C and a 12-hour light-dark cycle.

2.2.2 Study design

Allocation and treatment of animals

Animals were randomly divided into three groups as follows; ethanol group, saline controls and untreated controls (Fig. 2.1). The ethanol group (n=6) received 0.015ml/kg body weight of 25.2% ethanol once daily for 19 days via oral gavage from the first day of gestation (Fig. 2.2). This period covered the equivalent of first and second trimester in human during which most stages of bone development occur. The appearance of vaginal plug was considered day one of gestation. With respect to controls, the saline control group (n=6) received 0.015ml/kg body weight of 0.9% saline via the same route and for the same duration. The untreated control group (n=3) received neither alcohol nor saline. Fewer animals were used in the latter group to reduce the number of animals used in the study.

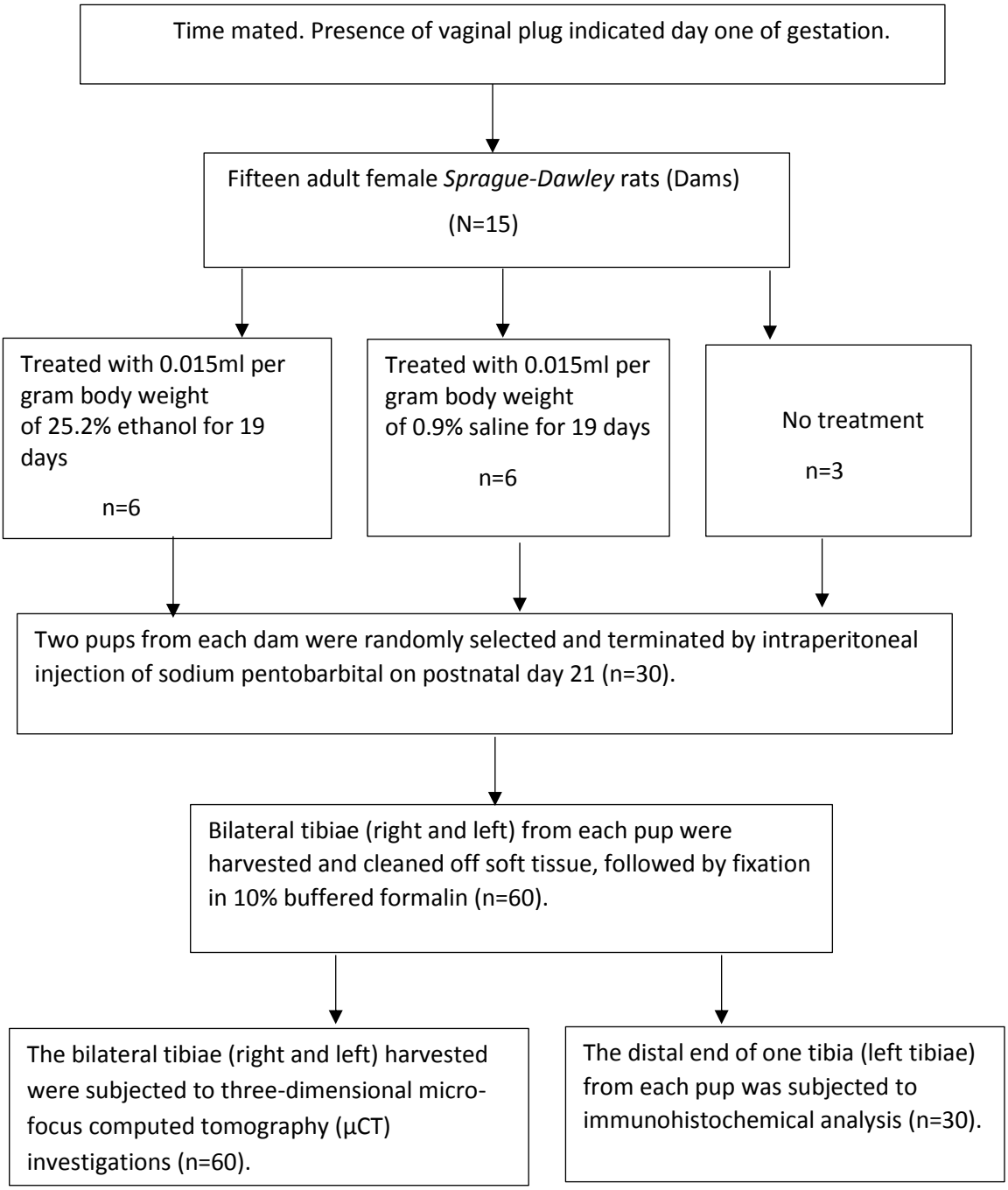

Figure 2.1: Conceptual study design.

To monitor growth and general health, the dams were weighed daily at approximately 10h00 using an electronic weighing scale (Snowrex Electronic Scale, Clover Scales, Pty,

Model-WP OO3, Johannesburg). Daily food consumption was also measured. Food consumed was determined by subtracting the weight of the food remaining in the feeding trough from the weight of the food given the previous morning. To determine peak blood ethanol concentration, tail vein blood samples were collected weekly, an hour after oral gavage.

Figure 2.2: process of oral gavage. The animal was held gently by grasping the loose skin on the back and the neck. A gavage needle was passed along the side of the mouth into the esophagus and towards the stomach. The solution was then gently passed directly in to the stomach (Image courtesy of R. Ndou).

Birth and termination of pups

The birth day of the pups in each litter was designated as day zero. The litter size was recorded upon birth and the pups were allowed to nurse freely with their dams for 21 days.

Upon reaching this age (21 days), two pups (n=30) from each of the dams (n=15) were randomly selected, weighed and crown rump length measured. The pups were then terminated by an intraperitoneal anesthetic injection of sodium pentobarbital. A thoraco-pelvic midline abdominal incision was made and slits were made on the skin covering the limbs to allow penetration of the fixative. Then the entire carcass was immediately immersed in freshly prepared 10% buffered formalin (Appendix 3) prior to dissection of the limbs.

Tissue harvesting

Bilateral hind limbs were carefully dissected and detached from the acetabulum using a pair of scissors, forceps and scalpel blade which were also used to excise all non-bony tissues. Knee joints were disarticulated and tibiae were removed, cleaned and subsequently immersed in fresh 10% buffered formalin for 24 to 72 hours prior µCT scanning (see section 2.8) and subsequent tissue processing for histological analysis (see section.2.5).

Blood ethanol concentration analysis

Tail vein blood (100 to 200µl) was collected into heparinised capillary tubes (Modulohm Vitrex®). Each capillary tube was sealed with prestick on both ends to retain the blood. Then paper towel was used to wrap the capillary tube before placing them individually into plastic bottles. These blood samples were immediately placed on ice. Within an hour after collection, all samples were stored at -80^{o}C for preservation until analysis.

Microcapillary tubes were thawed to room temperature and spun in a microhaematocrit centrifuge (Haematokrit 210, SN 0031 386-04, Hettich, Germany) at 3000 rpm for 10 minutes. Plasma alcohol concentration was carried out using the BioVision Ethanol Colorimetric Assay Kit (BioVision incorporation, Milpitas, USA) according to the manufacturer's instructions. All reactions and readings were done in an alcohol-free environment using iMark Bio-rad Microplate Absorbance Reader (Bio-rad Laboratories Inc, USA, catalogue number 168-1130). The protocol followed is shown in appendix 4.

The BioVision Ethanol Colorimetric Assay kit provides rapid, simple, and sensitive method for accurate quantification of ethanol concentration in various samples such as serum, plasma, food, beverages and other growth media. The ethanol is acted upon by alcohol oxidase to generate hydrogen peroxide (H_2O_2) that subsequently reacts with the kit's probe to generate colour $\lambda max = 570$nm that was measured using a micro-plate reader. The kit detects alcohol levels of between 0.1 and 10mg/dl.

2.2.3 Bone decalcification

Left tibiae were rinsed in distilled water to remove excess formalin and then individually immersed in disodium ethylenedeamine tetraacetic acid (EDTA) approximately 20 times the bone volume for three weeks (Appendix 5). In the past, different solutions were used for decalcification which include: morse solution, 5% trichloroacetic acid, formic acid, and hydrochloric acid. These solutions were found to have negative effects on preservation of tissue morphology, antigenicity and DNA integrity. In contrast, EDTA is widely used in immunolocalisation because of its ability in tissue antigenicity

preservation. However, it requires a longer decalcification time taking several weeks or months (Castania et al., 2015).

2.2.4 Test for end point decalcification

To test for end point decalcification, 5ml of EDTA was withdrawn from under the specimen and placed in to a separate tube. About 10ml of ammonium oxalate was added to the same test tube. The mixture was left to stand overnight and then observed for presence of precipitate (Appendix 6). The absence of precipitate indicated complete decalcification of the respective bone. All bone samples were rinsed in slow running tap water for 30 minutes and then placed in fresh 10% buffered formalin for three weeks before subsequent processing.

2.2.5 Bone length measurement

Prior to processing, the length of the individual bones was measured using a Digital caliper (series 530). The use of digital caliper provides simple and accurate measurement of 0.01mm or even better. Bone tissue was placed in a flat surface and the two internal jaws of the caliper slightly touching the proximal and distal ends of the bone as the reference points. Each measurement was repeated until a consistent result was achieved. The value was then divided into three equal parts representing the length of the shaft, proximal and distal ends. The exact length of the distal end was measured and carefully separated from the shaft for subsequent processing and embedding.

2.3 TISSUE PROCESSING

The distal end of the tibiae was then processed overnight in an automated tissue processor (Shandon Citadel 1000) as follows: fixation in 10% buffered formalin for 4 hours, dehydration in 70% alcohol each for 1 hour, in 3 changes of 95% alcohol for 2 hours each, in 3 changes of 100% alcohol for 2 hours each, in 2 changes of chloroform for 2 hours each and then impregnation in two changes of paraffin wax for 2 hours each (Appendix 7).

2.3.1 Paraffin wax embedding

Tissue samples were then embedded in paraffin wax making sure that the anterior surface of the distal end of the tibia was aligned in contact with the floor of the mold using forceps. The embedding wax, forceps and the molds were preheated at a temperature of 60^{o}C. Tissue samples were positioned in the metal molds, filled with molten wax and then covered with well-labelled plastic cassettes. The wax blocks were then allowed to cool on a frosted surface for about 20 minutes (Appendix 8), before they were detached from the molds.

2.3.2 Microtome serial sectioning

Excess wax surrounding the block was trimmed using a blade. When trimming, care was taken to ascertain that the upper and lower horizontal edges were parallel to each other. The blocks were then trimmed to the level of the tissue with the microtome (miles scientific, serial number 31602-554). One corner was stripped off to keep the ribbon straight during sectioning and to recognise the leading end of the ribbon (Fig. 2.3).

The blocks were precooled on ice before cutting 5µm thick sections. A ribbon of 9 sections was cut after discarding the first 20 sections. The ribbons of wax sections floated in a preheated water bath at 45^{o}C to flatten tissue section

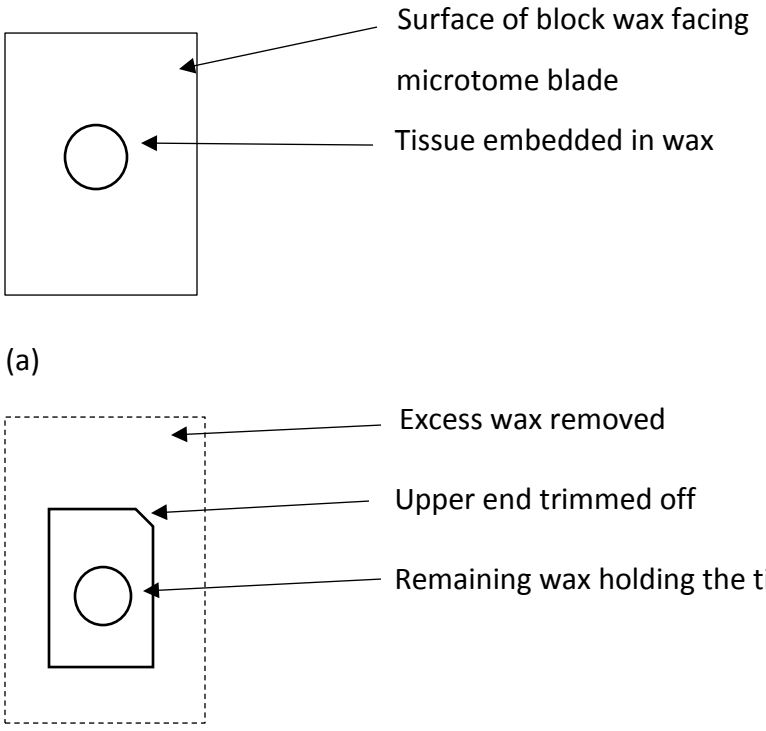

Figure 2.3: Trimming of wax blocks: (a) Shows the surface of wax block facing the microtome blade before trimming. (b) Excess wax removed and upper left corner trimmed off to determine the leading end of the ribbon.

Once flattened in the water bath, the sections were separated with forceps. The individual sections where then mounted onto silane coated microscope glass slides in a sequential order (Fig. 2.4).

The first section was stained with hematoxylin and eosin (H&E), whereas every alternate second and third section was immunolabeled with the anti Ki-67 antibody and its negative control, respectively. This process was repeated after discarding the next 20 sections resulting in each experiment done in duplicate.

Slides were allowed to dry at room temperature and then stored in an oven at 37^{o}C**.** The oven heated the slides and melted the wax surrounding the tissues and allowed the sections to further dry until when respective stain was conducted.

1	2	3	4	5	6	7	8	9
H&E	Ki-67	Neg	H&E	Ki-67	Neg	H&E	Ki-67	Neg

(a)

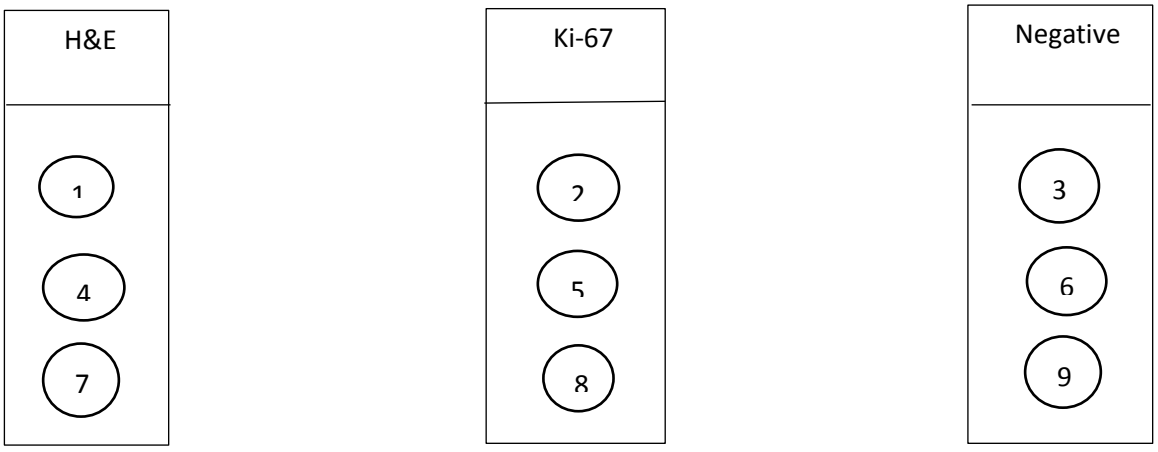

(b)

Figure 2.4: Serial sectioning of tissue (a) Shows the manner in which ribbons were serially sectioned **(b)** Shows the way in which slides were labelled and sections were picked.

The use of silane coated slides allowed an increased adhesive property of the tissue sections to the slides. The microscope slides were coated as follows: slides were arranged in a rack and completely immersed in 2% 3-aminopropyltriexothysilane (APES) for 30 minutes, rinsed in 2 changes of acetone for 10 dips, rinsed in 2 changes of distilled water for 10 dips, and then air dried at a 45^0 angle. Slides were then incubated in an incubator (model 508-2U, Labcon shaker) overnight at 37^0 (Appendix 9).

2.4 STAINING OF TISSUE SECTIONS

2.4.1 Haematoxylin and eosin staining

The haematoxylin and eosin stain is used to determine the architectural organization of tissue. Haematoxylin has the ability to stain the nuclei blue/black, while the eosin gives cytoplasm and connective tissue a pinkish and red colours respectively. This differentiates between the nuclear and non-nuclear components of the cell. In brief**,** sections were initially dewaxed in xylene for 2x 10 minutes and rehydrated by passing them through series of decreasing alcohol concentration (100%, 95%, and 70%) for 3 minutes each, and eventually rinsed in distilled water for 5 minutes. The sections were then stained with haematoxylin for 10 minutes, washed in running tap water for 2 minutes, differentiated in periodic acid for 2 dips, rinsed in slow running tap water for 2 minutes, blued in Scott's tap water for 2 minutes and then rinsed again in tap water for 10 minutes. Sections were stained with eosin for 2 minutes for cytoplasm staining and then dehydrated with increasing concentration of ethanol (70%, 95%, and 100%) for 3 minutes each, cleared in 2 changes of xylene for 10 minutes each and finally mounted in entellen (Appendix 10.1).

Use of Scott's tap water as a bluing agent has been found to be associated with gentle and smooth bluing of haematoxylin and decrease loss of tissue sections. The water was prepared by dissolving 2g of sodium hydrogen carbonate and 10g of magnesium sulphate in one litter of distilled water. The solutions were then stored in room temperature (Appendix 10.2).

2.4.2 Detection of cellular proliferation

Cellular proliferation remains an important tool in the study of many physiological and pathological processess. Biological methods have been used to explain various activities involved in different phases of cell cycle or proliferation. These methods can be broadly classified under DNA content analysis and immunohistochmeical methods (Hall and Levison, 1990).

2.4.2.1 DNA content analysis

DNA synthesis occurs during the S phase of the cell cycle and relies on incorporation of the precursors mainly pyrimidine deoxynucleoside to form the daugter DNA. Chemical staining of these precursors can be achieved, thereby assessing the rate of DNA replication. These methods include: thymidine labelling (incorporation) and tetrazolium-based colorimetric assay (Salic and Mitchison, 2008).

2.4.2.2 Immunohistochemical methods

Bromodeoxyuridine incorporation

Bromodeoxyuridine is a synthetic analogue of thymidine commonly used to detect DNA synthesis during the S phase of cell cycle (Hall and Levison, 1990). Bromodeoxyuridine is incorporated into the replicating DNA in the place of thymidine (5-iodo-2'-deoxyuridine). Anti BrdU antibodies can subsequently be used, thereby detecting an actively replicating DNA (Konishi et al., 2011).

Althogh the technique is widely used for detection of cellular proliferation, it is time consuming, expensive and radioactive making it not suitable for tissue incubation (Yu et

al., 1992). Moreover, tissues needs to be subjected to strong denaturation using concentrated hydrochloric acid or mixture of methanol and acetic acid. This may cause tissue destruction and decrease the intensity of bromodeoxyuridine (Salic and Mitchison, 2008).

Anti-Ki-67 antibody

Ki-67 is a nuclear antigen (Brown and Gatter, 1990) that is expressed by the proliferating cells during all the phases of cell cycle except the G_0 phase (Gerdes et al., 1984). The expression increases during the later half of S phase reaching its maximum at G2 and M phases of the cycle (Sasaki et al., 1987; Landberg et al., 1990; Bruno and Darzynkiewicz, 1992).

Previous studies show the anti Ki-67 antibody to have been used in detecting cellular proliferation in neoplastic and non neoplastic conditions; lymphoproliferative diseases, CNS tumours, connective tissue tumours and breast disease (Brown and Gatter, 1990). Likewise, the antibody was used to detect the presence of Ki-67 antigen secreted by various tissue components of the growing human long bones (Apte, 1990). Detection of the Ki-67 antigen is found to be most effective on frozencryostat sections. Thus, a heat induced atigen retreval step is therefore needed to effectively expose the epitope from protein complexes formed in formalin fixed tissue (McCormick et al., 2002). The use of anti Ki-67 antibody is a widely accepted immunohistochemical method of detecting cellular proliferation for the following reasons:

1. It is a direct, rapid and cost effective method of determining cellular proliferation (Hitchcock, 1991).

2. Ki-67 antigen is expressed specifically by actively proliferating cells. Therefore, the antibody plays a central role for detecting cellular proliferation (Brown and Gatter, 1990). Its usefullness as a tumour marker has to be tested for each tomour type and usage (Scholzen and Gerdes, 2000).

3. Ki-67 antibody is easily catalysed having a shorter half-life, thereby making it a strongly accepted marker of proliferation when compared to general markers (Bruno and Darzynkiewicz, 1992).

2.4.3 Immunohistochemistry

Chondrocytes proliferation is crucial in bone development. The anti-Ki-67 antibody (ab6246212 abcam) has received much larger attention as a marker for cellular proliferation. The antibody was found to be reactive with a nuclear structure present only in proliferating cells. The procedure was carried out over three days using the Rabbit Specific HPR/DAB (ABC) detection IHC kit (ab624621 abcam) as per manufacturer's instructions. The first day of the procedure involved dewaxing (2x 5 minutes) and rehydrating the tissue sections, washing tissue sections in running tap water for 5 minutes. The slides were then immersed in staining rack filled with citrate buffer solution (pH=6) and allowed to stay overnight in water bath (model number 416, serial number SE 9455) set at temperature of 60^0C. The high temperature and calcium chelating by citrate destroys the protein complex formation in formalin fixed tissue thereby

unmasking the specific epitopes within the protein molecules for effective antigen-antibody reaction (Shi et al., 2001).

The second day, tissue sections were allowed to cool to room temperature for 20 minutes and then washed in phosphate buffer solution (PBS) (pH=7.4) for 5 minutes. Endogenous peroxidase was blocked with 1% hydrogen peroxide (H_2O_2), washed with PBS for 3x 5 minutes, incubated with normal goat serum for 10 minutes, incubated with primary antibody (ki-67 in 1:1200 dilution factor) overnight at 4^0C. Endogenous peroxidase is an enzyme (produced by most tissues) that can produce nonspecific staining background. Although the enzyme activity is known to be destroyed during fixation, treatment of tissue section with 1% H_2O_2 will further reduce or completely abolish the nonspecific staining background (Ramos-Vara, 2005).

The third day, sections were allowed to reach room temperature, washed in PBS for 3x 5 minutes, incubated with biotinylated secondary antibody, washed in PBS for 3x 5 minutes, incubated with strep avidin HRP, washed in PBS for 3x 5 minutes. Sections were then incubated with DAB (3-3' di-amino benzidine) working solution for 5 minutes, rinsed in running tap water for 5 minutes, hydrated through graded alcohol, cleared in xylene and eventually mounted in entellen (Appendix 10.3).

Use of strep avidin in immunohistochemical staining has been shown to inhibit the action of biotin. Biotin is widely produced by many tissues including bones and can produce nonspecific staining background. It can also bind to the antibodies or the enzyme epitopes used in detecting target antigen. Strep avidin has high affinity to the biotin

thereby inhibiting the interaction and abolishing the nonspecific staining background (Ramos-Vara, 2005).

2.5 IMAGING MODALITIES

Different imaging mordalities for the assessment of skeletal morphology and microstructure exist. These include: plannar radiography, peripheral dual-energy X-ray absorptiometry, peripheral quantitative computed tomography, magnetic resonance imaging, synchrontron radiation and μCT (Christiansen and Bouxsein, 2013). The latter has become the goal standard imaging technique in assessment of bone microarchitecture (Bouxsein et al., 2010).

2.5.1 Peripheral dual x-ray absorptiometry

Peripheral dual x-ray absorptiometry (pDXA) involves exposing the specimen to two sources of energy beams: low and high energy beams. The ratio of the two energy beam's attenuation allows the separation of bone from soft tissue and fat (Christiansen and Bouxsein, 2013). Measurements of body composition and skeletal structure using pDXA is associated with some limitations which include: poor accuracy, underestimation of lean tissue mass and overestimation of fat mass (Nagy and Clair, 2000; Brommage, 2003). Despite efforts by few investigators to standardise the measurements, the technique is generally associated with limited spatial resolution, assessment of areal two-dimensional bone marrow density rather than volumetric and an inability to delineate between trabecular and cortical bone compartments (Christiansen and Bouxsein, 2013).

2.5.2 Magnetic resonance imaging

Magnetic resonance imaging is widely used to assess bone microstructure based on the strong magnetic fields. It is a non-invasive and nonionizing technique (Genant and Jiang, 2006). Bone tissue gives a weak micro resonance signal due to lack of protons, whereas soft tissues produces strong micro resonance signals due to the presence of protons. This contrast allows easy delineation and quantification of trabecular bone structure (Jiang et al., 2000; Christiansen and Bouxsein, 2013). Certain limitations affect *in vivo* detection of trabecular bone in smaller animals (Jiang et al., 2000). These limitations include: spatial resolution, total imaging time and limitations of signal-to noise. However, images can show network of larger trabeculae (Genant and Jiang, 2006).

2.5.3 Microcomputed tomography

Microcomputed tomography (μCT) was developed by Feldkamp and colleagues in late 80's and is recently the gold standard technique in assessing the microarchitecture of bone. The resolution allows clear visualisation of individual smaller trabeculae. When using μCT, it is easy to directly quantify the trabecular structure such as trabecular volume, number, thickness, and separations (Genant and Jiang, 2006; Bouxsein et al., 2010).

Studies have shown that μCT is relatavely more accurate in assessing trabecular bone strucuture compared with other imaging modalities (Kapadia et al., 1998; Barbier et al., 1999; Waarsing et al., 2004; Bonnet et al., 2009). However, a study reported an overestimate of the trabecular measuremets (trabecular bone volume, trabecular

thickness and separation) relative to histomorphometric analysis. This may be attributed to the choice of inadequate resolution relative to trabecular size and poor threshold selection. Moreover, measurements on trabecular nodes tend to increase trabecular thickness compared to the measurement on trabecular struts (Chappard et al., 2005).

Advantages of using Micro Computed tomography

Despite above mentioned limitations of using µCT, it has several advantages making it suitable over other imaging modalities:

1. It allows direct three-dimensional measurement of trabecular number, thickness, and separations rather than assumption based on two-dimensional stereological method (Hildebrand and Rüegsegger, 1997).

2. It is fast, precise and non-destructive. The specimen can be used subsequently for further assay (Rüegsegger et al., 1996).

3. Much larger volume of interest can be analysed (Bouxsein et al., 2010).

4. By comparing material attenuation to that of known, µCT can provide an estimate of bone tissue mineralisation (Fajardo et al., 2009).

2.5.4 Light microscopy and photomicrography

Photomicrographs of the stained slides were taken under light microscope (Zeiss Axioscope 2 plus) fitted with an axiocam HRC digital camera (identification number 105-041756). Photomicrographs of the medial, lateral and central region of each section were taken under ×10 magnification for assessment of chondrocyte number, cellular

proliferation and areas of the different chondrocytes zones (proliferative and hypertrophic) of the distal growth plates.

Photomicrographs were imported into Fiji Image-J software and the parameters measured were delineated based on cell morphology. The proliferative zone is limited by the first flattened chondrocyte on the bottom side and the first hypertrophic chondrocytes on the upper side. Whilst the hypertrophic zone is limited by the first hypertrophic chondrocytes from the bottom side and by the last transverse septum on the upper side (Fig. 2.5). Absolute parameters assessed include the following: cell count, cellular area, growth plate area, as well as cellular proliferation.

Cell count

Cell count was determined as the average number of cells within each zone of the growth plate (proliferative and hypertrophic zone) as follows: images were converted to greyscale (8-bit) after which the area of the cells to be counted were highlighted. This was done using the "set" button in image-J to type in a known pixel intensity thereby creating a binary version of the image with two pixel intensities: black = 0 and white = 255. For merged cells, process > binary > watershed, and fill holes was used to accurately separate them by adding one-pixel cell line and fill holes respectively. The menu command (process > binary > watershed) convert the image to binary by thresholding. The black pixels are then replace with a grey pixels with black pixels closer to the edge lighter than the black pixels that are more central. This is the Euclidian distance map of the black area from which the centre of the particles are calculated. They are the

ultimate eroded area of each black area which is equivalent from each area, the points are then dilated until they touch another black pixel. The meeting point is where a watershed line is drawn. The region of interest (ROI) was selected and particles were analysed. To count all the particles, the Image J setting was adjusted to the default of 0-infinity. Finally, clicking an outline option shows a copy of the image and all counted particles as well as the cellular area were shown in numbered outlines (Appendix 11).

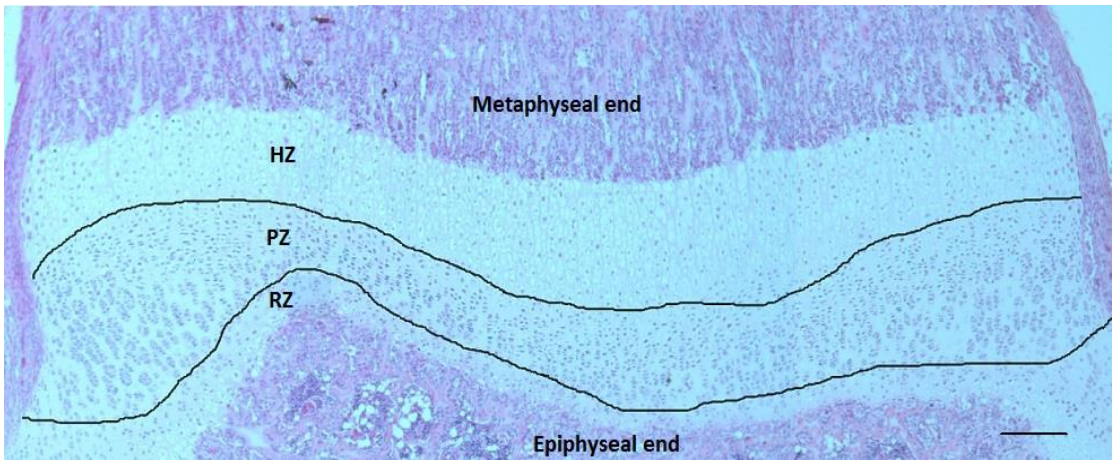

Figure 2.5: **Photomicrograph of the growth plate (distal end) showing the proliferative and hypertrophic zones.** Proliferative zone (PZ) and hypertrophic zone (HZ) areas (irregular lines) are delineated. Haematoxylin and eosin (Image courtesy of Bello NK and Perry V).

Cellular area

Cellular area was determined as the average sum of the areas occupied by the cells in each zone (proliferative and hypertrophic zone) as explained above.

Growth plate area

Growth plate area was determined as the average sum of the resting, proliferative and hypertrophic zones areas. Following the automated routine threshold setting as explained above, the entire growth plate area was selected using a polygonal selection tool. An outline of the analysed area was drawn.

Cellular proliferation

Cellular proliferation was determined as the average number of Ki-67 positive cells within the proliferative and hypertrophic zones of the growth plate as described above.

2.5.5 Three-dimensional micro-focus x-ray computed tomography

Recently, high-resolution three dimensional (3D) imaging technique has received much attention in evaluating bone morphology and microarchitecture. It involves the use of X-ray attenuated data that is acquired at multiple viewing angles to reconstruct a 3D representation of the specimen. The accuracy and non-destructive advantages of assessing bone morphometry by μCT makes the specimen useful for other subsequent assays (Bouxsein et al., 2010).

Microfocus computed tomography x-ray machine (NIKON XTH 225/320 LC) was used in this study. The samples preserved in 10% buffered formalin were first freed of excess fluid by patting around the bone with a paper towel prior to scanning. The bones where then individually wrapped in Styrofoam and placed in a plastic container. Wrapping Styrofoam around the bone ensured that the sample remained stationary during scanning while allowing the X-rays to get to the sample with negligible absorption. The plastic container with the sample inside was then positioned on a rotating manipulator in the scanning chamber for the scanning. The scanning parameters used are shown in table 2.1.

Parts of the tibia studied

The full bone length was measured using the VG studio built in calliper. Cross-sectional area, cortical area and medullary canal area of the shaft were measured at two positions, 50th (midshaft) and 75th (distal) percentile marks of the tibial length (Fig. 2.6). These

points were determined by dividing the bone length into quartiles. From the midshaft, the circumference was also taken.

Table 2.1: Scanning parameters

Parameter	Value
X-ray voltage	70kv
X-ray current	400µa
Filter	1mm aluminium
Scanning resolution	15µm
Tomographic rotation	360 degrees
Rotation step	1 degree
Frame averaging	4
Scan duration	8 minutes

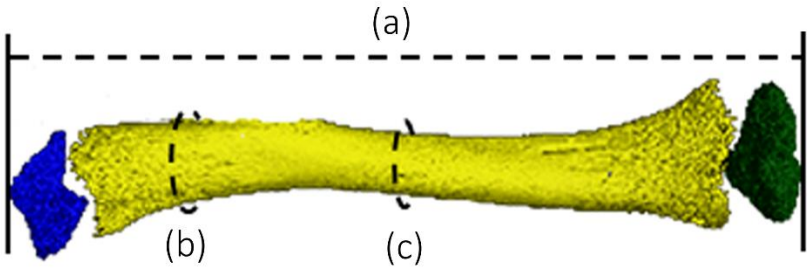

Figure 2.6: Three-dimensional reconstruction of the tibia showing the parts that were investigated. (a), full tibial length; (b), 75th percentile mark; (c), 50th percentile mark (midshaft). The blue part represents the distal epiphysis in which trabecular morphometrics were studied. The yellow part is the shaft (Image courtesy of R. Ndou).

Table 2.2: Trabecular parameters assessed

Parameters	Abbreviation	Definition
Bone volume to total volume	BV/TV	Represents the ratio of material (bone) to total volume.
Mean trabecular thickness	TbTh	Specifies the mean thickness of trabecular (column-like) structures in the material (bone), calculated as follows: $\mathrm{TbTh} = (2/\mathrm{BS})/\mathrm{BV}$ Where BS/BV is the ratio of material (bone) surface (BS) to material (bone) volume (BV).
Trabecular number	TbN	Shows the mean number of trabecular (column- like) structures per unit length, calculated as follows: $\mathrm{TbN}(\mathrm{BV}/\mathrm{TTTbTh}$
Mean trabecular spacing	TbSp	Indicates the mean distance between Trabecular (column-like) structures, calculated as follows: $\mathrm{TbSp} = 1/\mathrm{TbN} - \mathrm{TbTh}$

Bone morphometry

Reconstruction was done using 3D Pro® after which, VG studio Max® 3.0 was used for data analysis. The gray values representing the container were excluded using the import histogram. On the preview, the parts representing air were also cut out to reduce computer memory processing power required during analysis. Care was taken to ensure the sample was not cut out. To ensure that only the bone material was being examined, manual surface determination was applied ascertaining that the background was removed without compromising the sample material of interest. The region of interest

was then selected for surface determination. After selecting the distal epiphysis as a region of interest, the trabecular number, thickness, spaces and volume were obtained under “morphometrics” on VG studio.

Osteometric measurements were obtained using the built-in caliper. The full bone length was divided to determine the midshaft and further divided into four to determine the quartile marks. A cross sectional slice from each quartile was then saved for further analysis on Fiji image J. From these slices, cross sectional circumference, cross sectional area and cortical thickness where obtained as described in appendix 12. Cortical thickness was the difference between the cross-sectional area and the medullary cavity area.

2.6 STATISTICS ANALYSIS

The data were managed in Microsoft Excel 2016 (Microsoft Corporation) and analysed using SPSS® version 24, IBM®, 2017. The Shapiro Wilks test was used to test for normality. Since the data were parametric, ANOVA with LSD post-hoc was used to test for group differences. Pearson's correlation was used to test for relationships between parameters. Binary logistic regression was used to predict group membership into either the ethanol or saline control group. The data are reported as mean ± standard deviation. Significance level was set at $p < 0.05$.

3 RESULTS

3.1 Measurement reliability

Lin's concordance correlation coefficient for intra and inter observer errors showed pc values above 0.7 for all measurements. Values for pc range from -1 to 1 and a value close to 1 indicates a high degree of measurement similarity. Greater than 0.7 pc values obtained herein indicate that the correlation between repeated measurements was high and thus measurement error was minimal.

3.2 Blood alcohol concentration

The mean blood ethanol concentration was 258.77mg/dL in the ethanol group and 81.53mg/dL in the saline controls. The untreated controls were not tested for blood ethanol concentration as they did not receive treatment.

3.3 Food consumed and weight gained during the gestation period

All three groups studied showed similar daily food consumption in each week. The food intake was highest in week 3 for all the groups, and was not significantly different between the groups ($p=0.75$ for ethanol vs saline control) (Fig. 3.1). With respect to the weight gained per week, the ethanol group showed a negligible gain from week 1 (28.3g) to week 2 (29.42g). In contrast, the saline and untreated controls exhibited a slight weight decrease from week 1 to week 2 (34.21g – 29.21g and 30.5g – 24.83g respectively). However, all the three groups showed a major weight increase from week 2 to week 3 (Fig. 3.2). The ethanol group had the least total weight gained for the entire gestation period (Fig. 3.3).

3.4 Gestation duration and litter size

The gestation duration ranged from 19 to 24 days (Table 3.1). This range was 21-24 days in the ethanol group and 19-23 days in the saline controls. The untreated controls had 23 days gestation. However, there were no statistical group differences in gestation duration (p=0.37 for ethanol vs saline control). There was a wide range of litter size among the three groups, with the smallest being 3 in the ethanol group and the largest observed in the untreated controls that had a maximum of 17 (Table 3.1). This group also had the smallest range of 14 -17. This contrasts with the ethanol group (litter size 3-16) and the saline controls (litter size 5-16). However, no significant differences were observed between the groups (p=0.28 for ethanol vs saline control). Each of the three groups in the study had 2 pups found dead at birth.

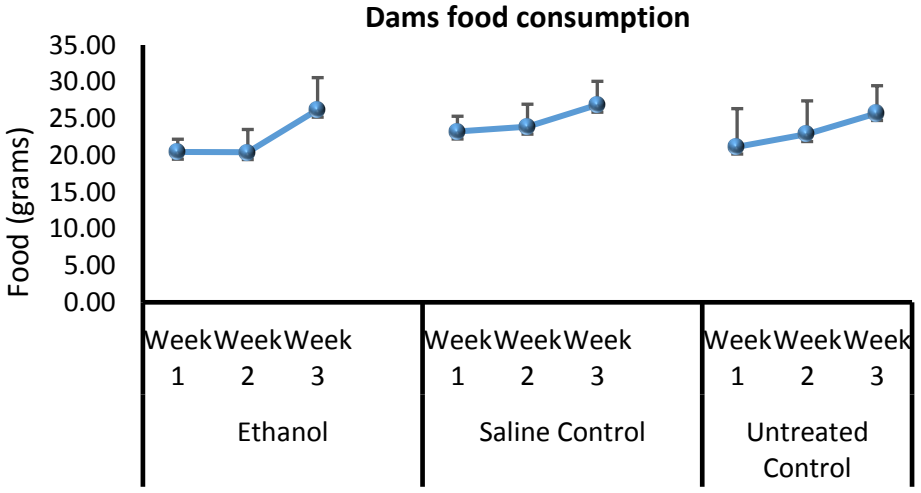

Figure 3.1: Food consumption. The daily food consumption in grams is shown as an average per week for all three groups in the study. Error bars represent standard deviation.

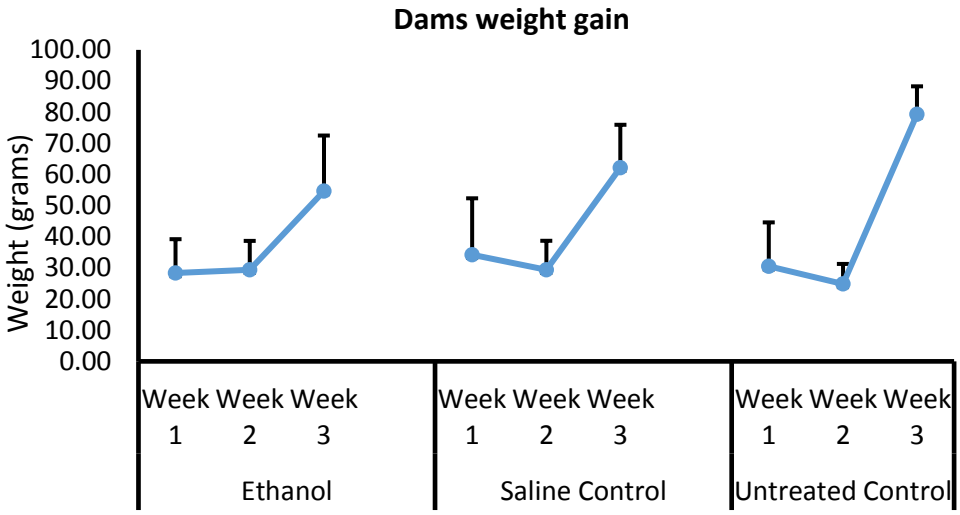

Figure 3.2: Weight gain. The weekly mean weight gained in grams is shown for all three groups in the study. Error bars represent standard deviation.

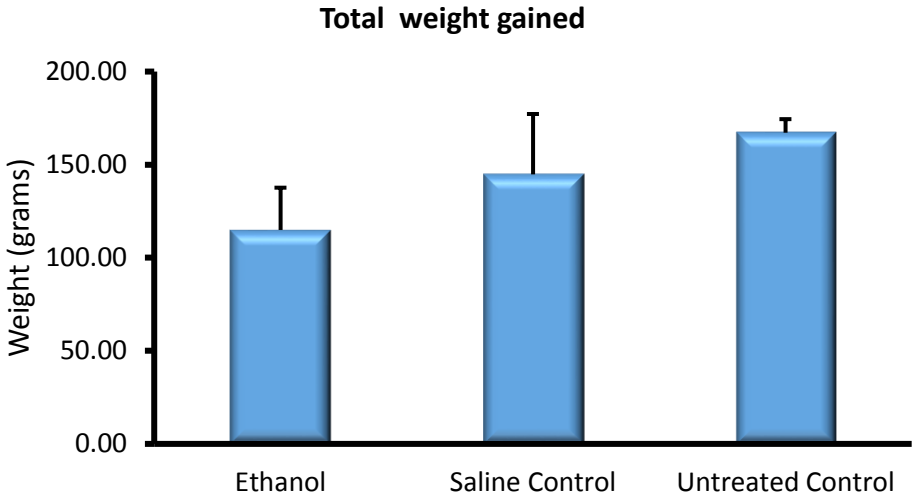

Figure 3.3: Overall weight gain. The total mean weight gained in grams for the entire gestation period is shown for all three groups in the study. Error bars represent standard deviation.

Table 3.1: Gestation duration and litter size for the ethanol group, saline and untreated controls. The number of dead pups (n = 2) in each group is included in litter size.

Group		N	Minimum	Maximum	Mean	SD
Ethanol	Gestation	6	21	24	23.00	1.095
	Litter size	6	3	16	9.83	4.916
Saline Control	Gestation	6	19	23	22.00	1.732
	Litter size	6	5	16	12.14	3.671
Untreated Control	Gestation	3	23	23	23.00	0.000
	Litter size	3	14	17	15.33	1.528

3.5 Pups weights and crown rump length at 3 weeks of age

Minor differences in the weight of the pups at the age of 3 weeks were observed. The ethanol group (47.41g) weighed marginally lower than the saline (48.20g) and untreated controls (50.83g) (Fig. 3.4). These differences were not statistically significant (p=0.45). The crown rump length was similar in the ethanol group and the saline controls (9.70cm), being significantly higher in the untreated control group (p=0.01 for untreated control against the ethanol and saline groups) (Fig. 3.5).

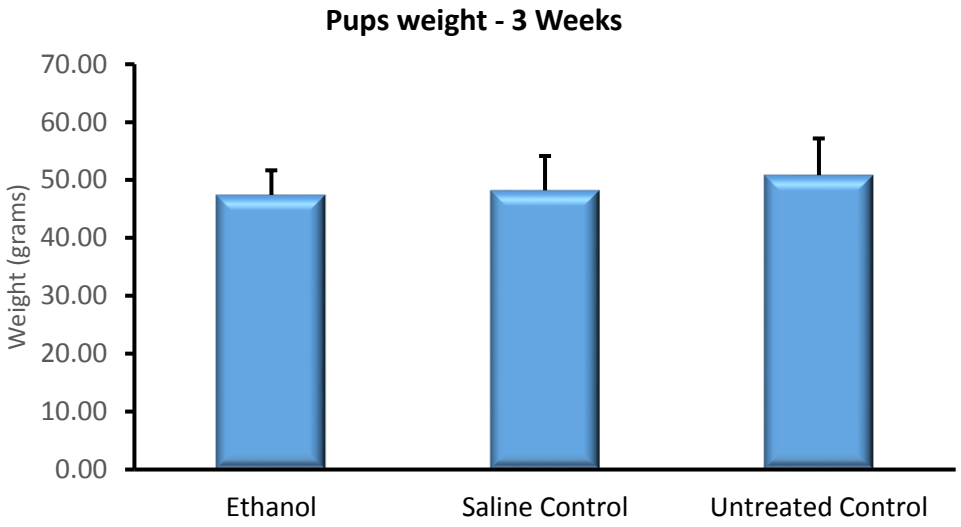

Figure 3.4: Weight of the pups at 3 weeks of age. The mean weight is given in grams for all three groups in the study. Error bars represent standard deviation.

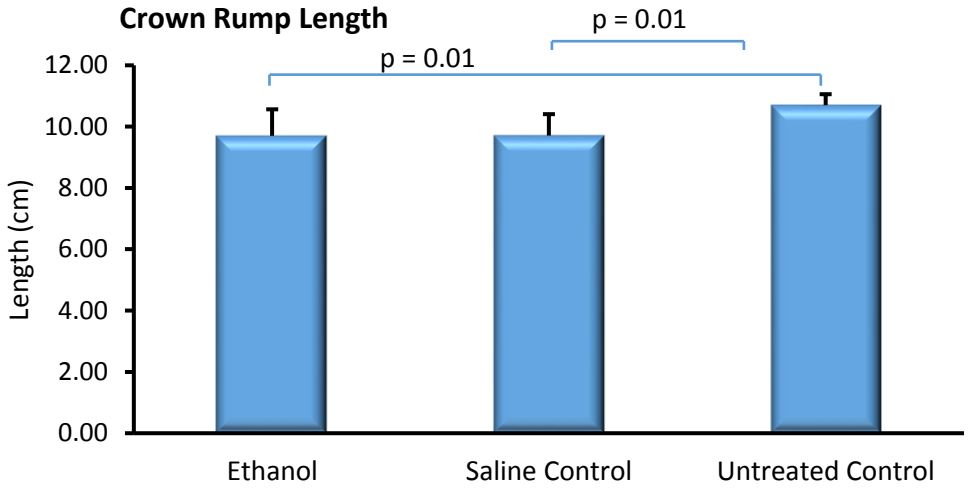

Figure 3.5: The crown rump length of the pups at 3 weeks of age. The values are means in grams for all three groups in the study. Error bars represent standard deviation. A line connects group with significance difference from the ethanol group.

3.6 Histomorphometry and immunohistochemistry for Ki-67 protein

Growth plate surface area

The growth plate surface area was smallest in the ethanol group (Mean=7.87mm^2 ±2.05) compared to the saline and untreated controls (Mean=9.09 mm^2 ±1.11 and 9.24 mm^2 ±1.05, respectively). However, no significant differences were observed among all three groups (p=0.05) (Fig. 3.6a).

Proliferative zone

The ethanol group exhibited fewer cells (Mean=1637.00 ±356.60) than the saline and untreated controls (Mean= 1808.56 ±742.88 and 2435.67±638.94, respectively). These cells were significantly fewer between the ethanol and the untreated group (p=0.03) (Fig. 3.6b). The ethanol group also had the smallest (Mean= 0.18 mm^2 ±0.06) proliferative zone surface area compared to the saline (Mean= 0.28 mm^2 ±0.18) and untreated controls (Mean= 0.27 mm^2 ±0.11). However, no significance differences were observed (p=0.05 for all group comparisons) (Fig. 3.6c). Similarly, fewer Ki-67 labelled cells were found in the ethanol group (Mean=1038.13 ±213.79) than the saline controls (Mean=1568.00 ±302.92) and untreated group (Mean=1484.75 ±200.65) (p=0.001 and 0.003, respectively) (Fig. 3.6d).

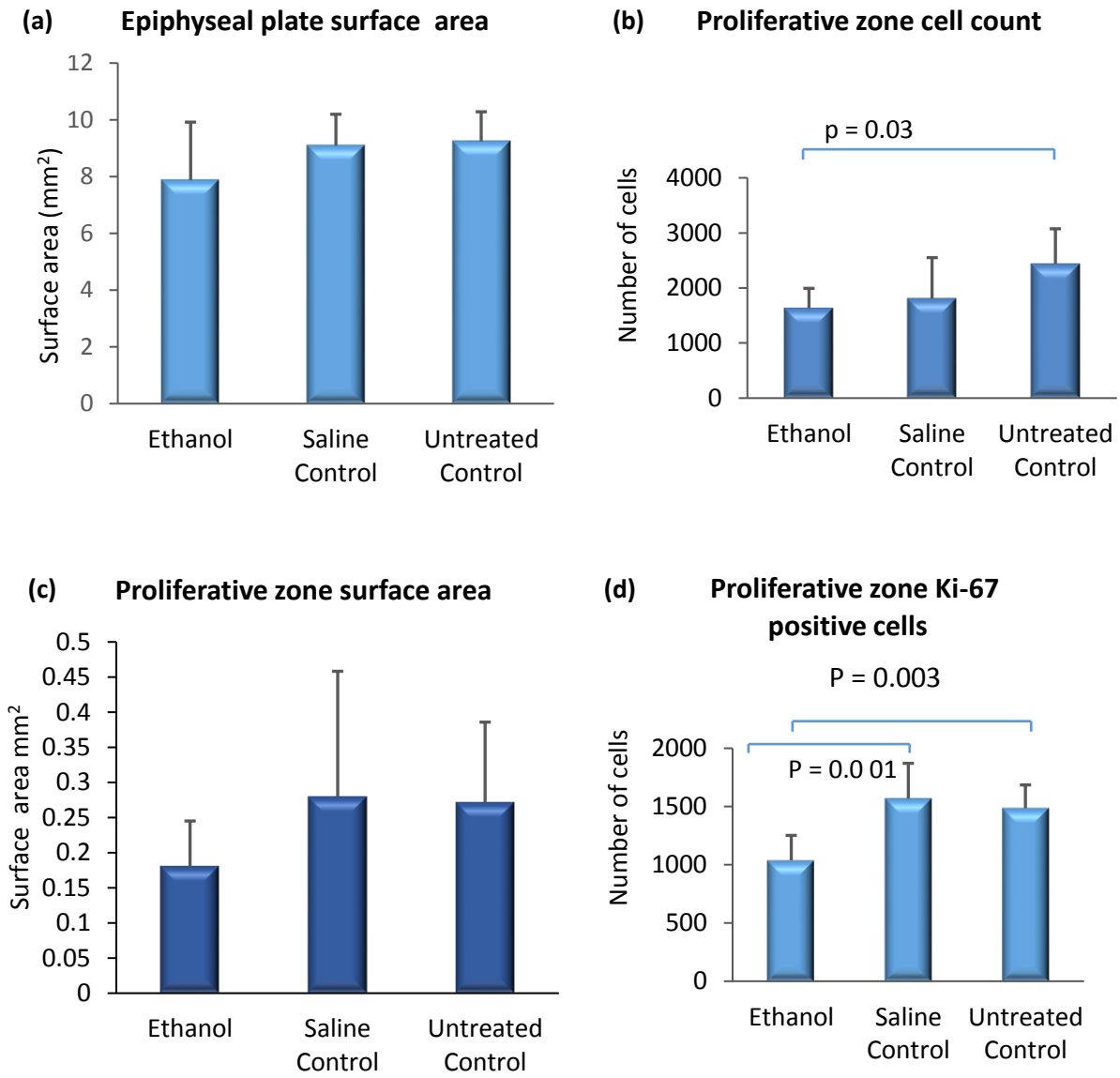

Figure 3.6: Histomorphometry and Ki-67 positive cells in the tibial distal epiphyseal plate. (a) epiphyseal surface area, (b) proliferative zone number of cells (c), proliferative zone surface area and (d) the number of Ki-67 positive cells in the proliferative zone are given for the ethanol, saline control and untreated control groups. Error bars represent standard deviation and a line connects bars with significant difference from the ethanol group.

Hypertrophic zone

In the hypertrophic zone, the ethanol group had fewer cells (Mean=1199.71 ±120.93) than the saline controls (Mean=1421.50 ±431.27) and the untreated group (Mean=1459.42 mm^2 ±146.34). However, no significant differences were observed ($p>0.05$ for all group comparisons) (Fig. 3.7a). The ethanol group also had the smallest (Mean=0.14mm^2 ±0.06) hypertrophic zone surface area compared to the saline (Mean=0.17 mm^2 ±0.05) and untreated controls (Mean=0.18 mm^2 ±0.02). However, no significant difference were observed from each other ($p=0.05$) (Fig. 3.7b). Similarly, fewer Ki-67 labelled cells were found in the ethanol group with significant differences observed only between the ethanol (Mean=1081.19 ±207.14) and the saline group (Mean=1157.25 ±232.37) ($p=0.003$) (Fig. 3.7c).

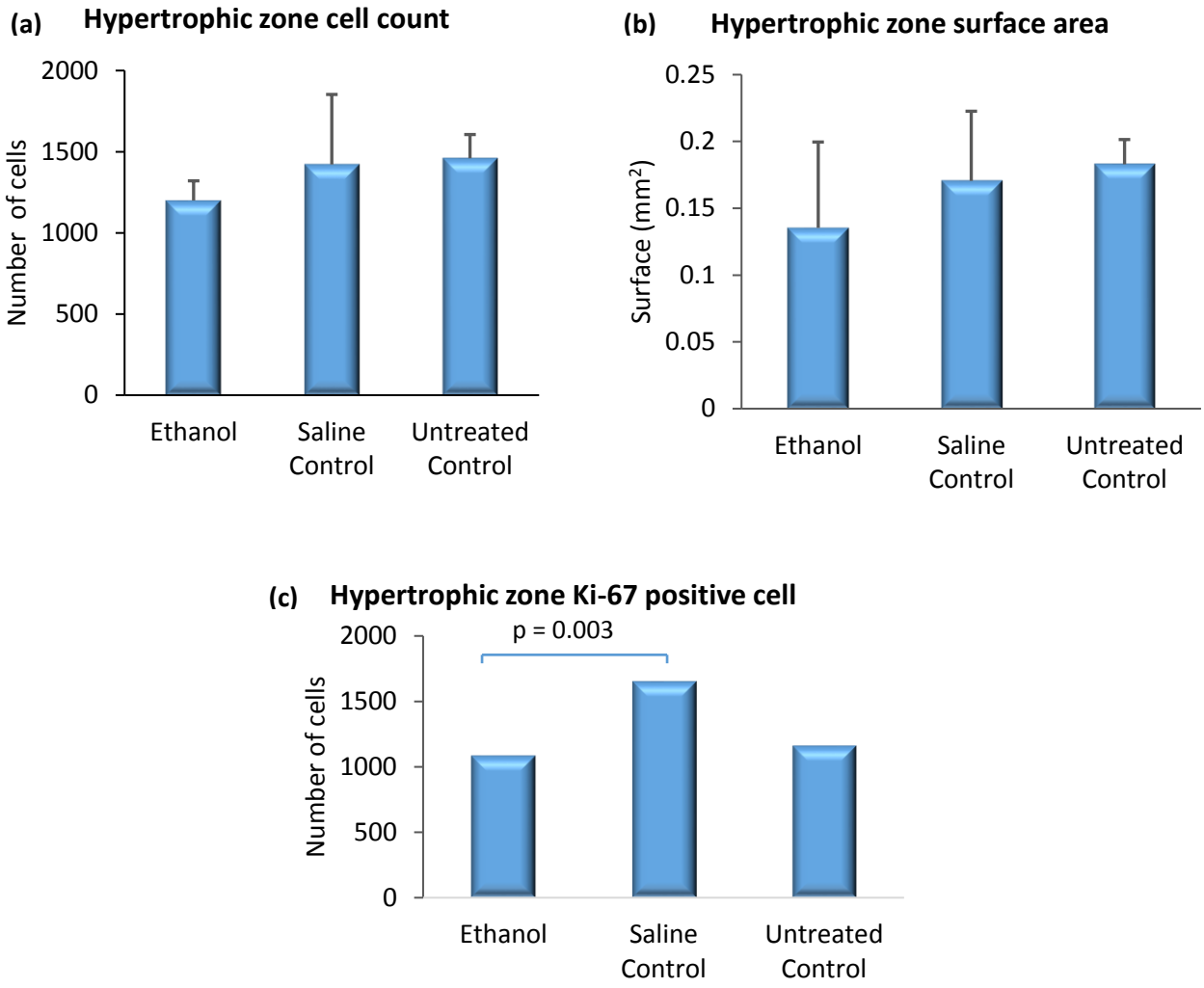

Figure 3.7: Histomorphometry and Ki-67 positive cells in the tibial distal epiphyseal plate hypertrophic zone. (a) hypertrophic zone number of cells, (b) hypertrophic zone surface area and (c) the number of Ki-67 positive cells in the hypertrophic zone are given for the ethanol, saline control and untreated control groups. Error bars represent standard deviation and a line connects group with significance difference from the ethanol group

3.7 Osteometry

The mean full bone length was similar in all three groups studied (ethanol, mean=21.08mm ±0.95; saline control, mean=21.23mm ±1.38 and untreated control, mean=21.88mm ±0.94) (Fig. 3.8a). This similarity among the groups was also observed in the shaft length. The mean shaft length for the ethanol group was 17.77mm ±0.92 and 17.51mm ±1.32 for the saline and untreated controls a mean of 18.22mm ±0.74 (Fig. 3.8b). In contrast, the distal volume showed differences between the study groups, with the ethanol group showing a significantly smaller volume (Mean=3.51mm^3 ±1.07) than the saline (Mean=4.35 mm^3 ±0.78) and untreated controls (Mean=4.26 mm^3 ±1.02) ($p=0.007$ and $p=0.04$ for the ethanol group compared to the saline and untreated groups respectively) (Fig. 3.8c).

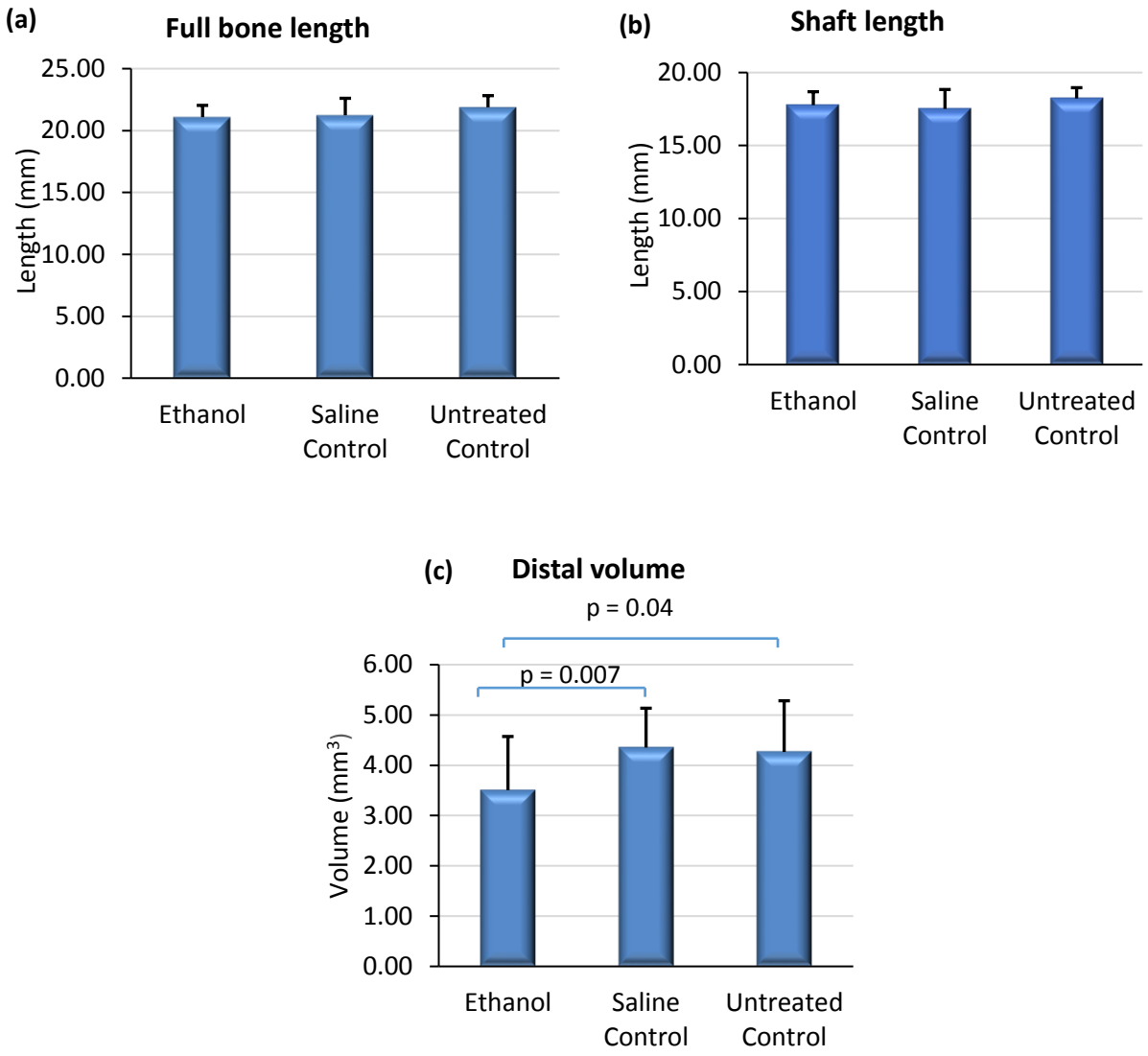

Figure: 3.8: Measurements and volume: (a) full bone length, (b) shaft length and (c) distal volume. All parameters are given for the ethanol, saline controls and untreated controls. Error bars represent standard deviation.

3.7.1 Trabecular parameters

The ethanol group (Mean=54.73% ±14.53) also had less bone to total volume (BT/TV) compared to the saline (Mean=66.81% ±11.05) and untreated controls (Mean=68.83% ±15.35) (Fig. 3.9a). This difference was significant for the ethanol and saline groups ($p<0.001$) with both control groups showing similarity ($p=0.38$). The ethanol group

(Mean= 0.14 ±0.10) showed the thinnest trabeculae (TbTh) of all three groups in the study, being significantly lower than the saline control (Mean= 0.20 ±0.08) (p=0.03) (Fig. 3.9b). The number of trabecular (TbN) was similar in all three groups (ethanol, mean=5.04 ±1.70; saline control mean=5.46 ±1.32 and untreated control mean=5.48 ±0.61) (Fig. 3.9c). However, differences in trabeculae spacing (TbSp) occurred, with the ethanol group (Mean=0.08mm ±0.04) displaying less spacing than the saline (Mean=0.13mm ±0.06) and untreated group (Mean=0.13mm ±0.06) (Fig. 3.9d). These differences were statistically significant for both the ethanol and untreated controls (p=0.002 and p=0.02 for the ethanol group compared to the saline and untreated groups respectively.

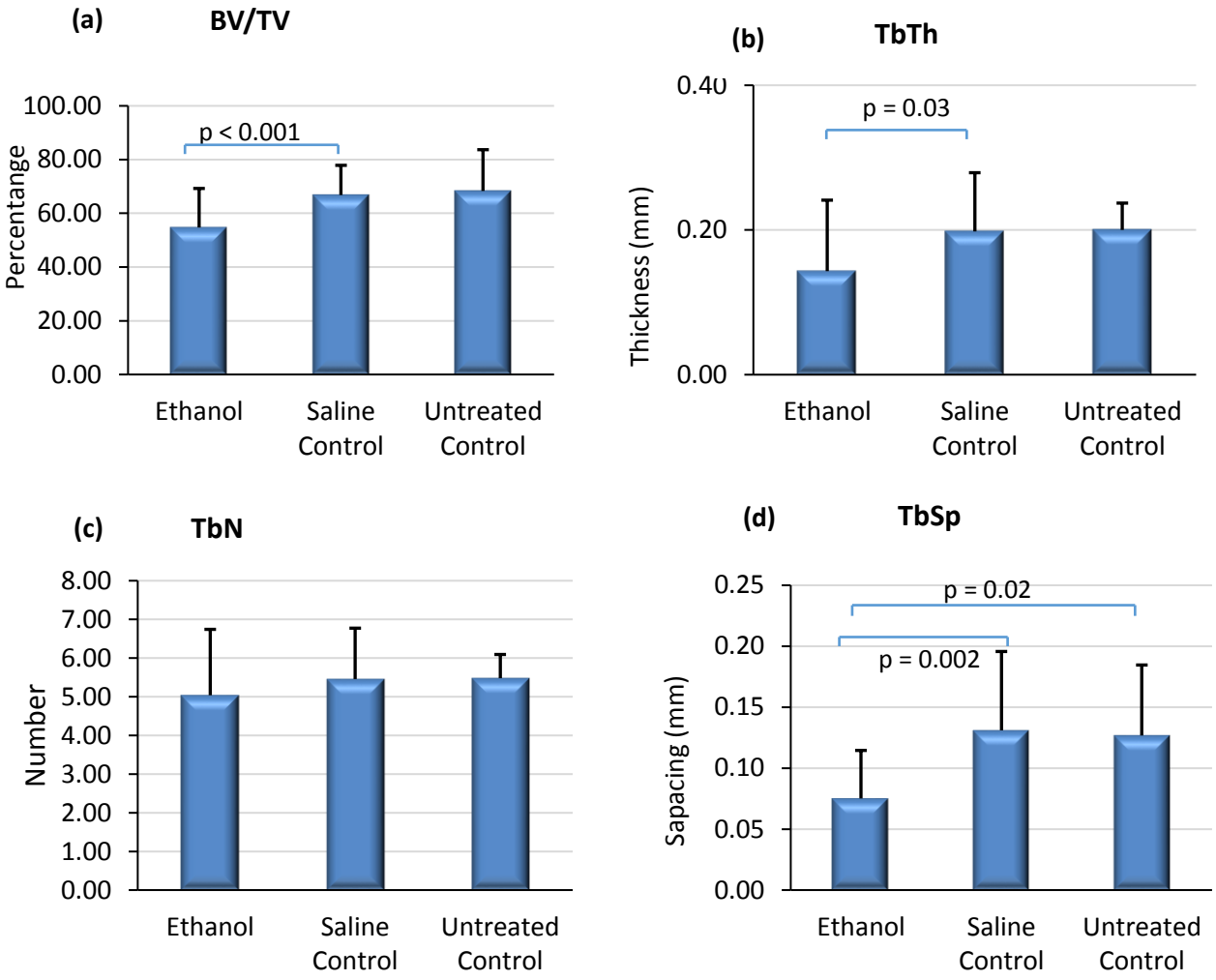

Figure 3.9: Trabecular morphometric parameters (a) bone volume to total volume (BV/TV), (b) trabecular thickness (TbTh), (c) trabecular number (TbN), (c) trabecular spacing (TbSp). All parameters are given for the ethanol, saline controls and untreated controls. Error bars represent standard deviation and a line connects group with significance difference from the ethanol group.

3.7.2 Midshaft cross-sectional area, cortical area (thickness) and medullary canal area

The midshaft cross sectional area was similar in all three groups studied. The ethanol group had mean of 2.48 mm^2 ±0.41 and the saline and untreated groups had 2.51 mm^2 ±0.37 and 2.45 mm^2 ±0.44, respectively (Fig. 3.10). The medullary canal area was greater in the ethanol group (1.01 mm^2 ±0.25) in comparison to the saline and untreated controls (Mean=0.96 mm^2 ±0.16 and 0.86^2 mm^2 ±0.12 respectively). Significant differences in medullary canal area where observed between the ethanol and untreated controls (p=0.05) (Fig. 3.11). Regarding cortical area (thickness) in this bone region, the ethanol group (Mean=1.47 mm^2 ±0.32) exhibited a marginally lower value compared to the saline and untreated controls which had the same size area (Mean=1.5 mm^2 ±0.25 and ±0.45, respectively) (Fig. 3.12).

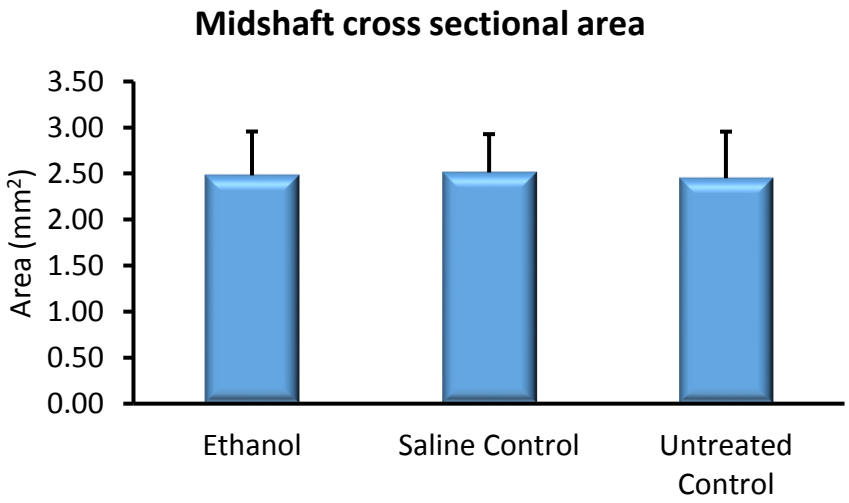

Figure 3.10: Midshaft cross-sectional area. The mean cortical area at the 50th percentile mark is given for the three groups studied. Error bars represent standard deviation.

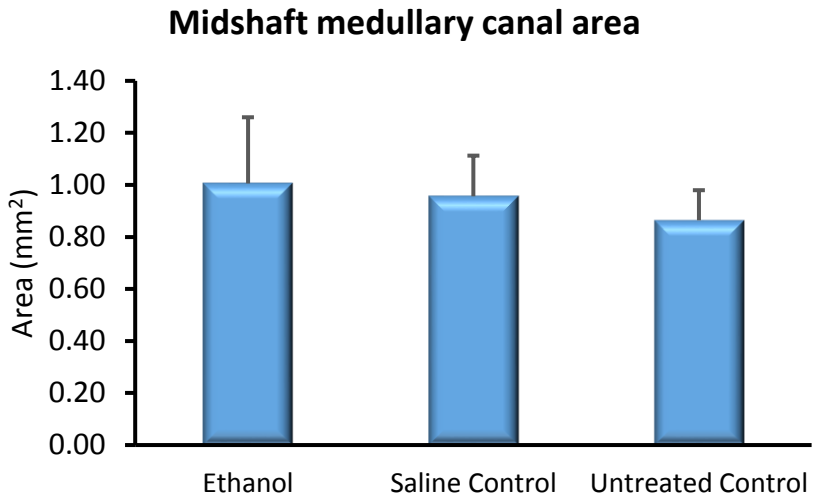

Figure 3.11: Midshaft medullary canal area. The mean medullary canal area at the 50th percentile mark is given for the three groups studied. Error bars represent standard deviation.

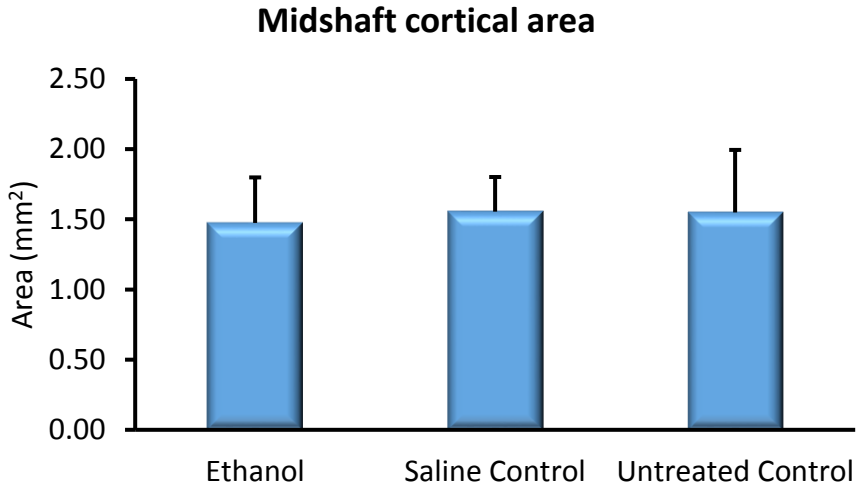

Figure 3.12: Midshaft cortical area. The mean medullary canal area at the 50th percentile mark is given for the three groups studied. Error bars represent standard deviation.

3.7.3 Distal cross-sectional area, cortical area (thickness) and medullary canal area

The distal cross-sectional area was marginally lower in the ethanol group (Mean=3.14 mm^2 ±0.56) compared to the saline and untreated controls (Mean=3.38 mm^2 ±0.62 and 3.45 mm^2 ±0.57, respectively). Although the ethanol group appeared to have a smaller cross-sectional area in this bone region, no significant difference were observed from the controls (p=1.15) (Fig. 3.13). The distal medullary canal appear small in the ethanol group (1.49 mm^2 ±0.35) in comparison to the saline and untreated controls (1.71 mm^2 ±0.38 and 1.82 mm^2 ±0.57, respectively). These differences were only significantly different between the ethanol group and untreated control (p=0.03) (Fig. 3.14). With respect to cortical area (thickness) in this bone region, the ethanol group (1.61 mm^2 ±0.34) exhibited a marginally lower value compared to the saline and untreated controls (1.66mm^2 ±0.89 and 1.63 mm^2 ±0.55, respectively). Again, no significant differences were observed (p=0.17) (Fig. 3.15).

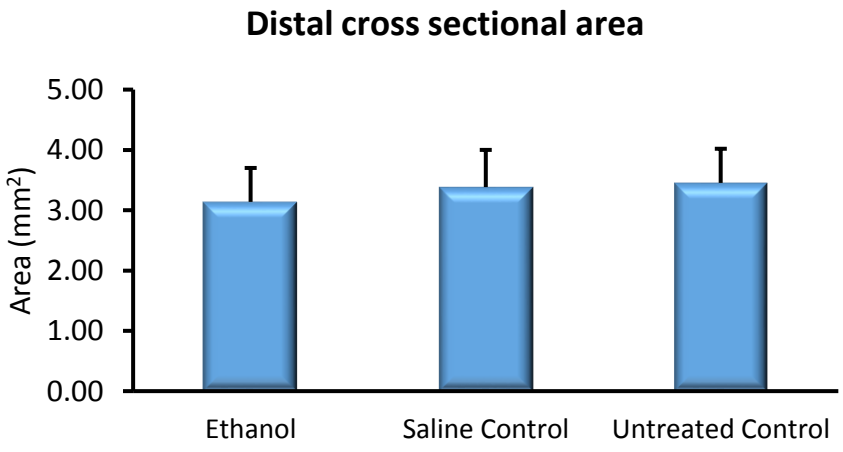

Figure 3.13: Distal cross sectional area. The mean cortical area at the 75th percentile mark is given for the three groups studied. Error bars represent standard deviation.

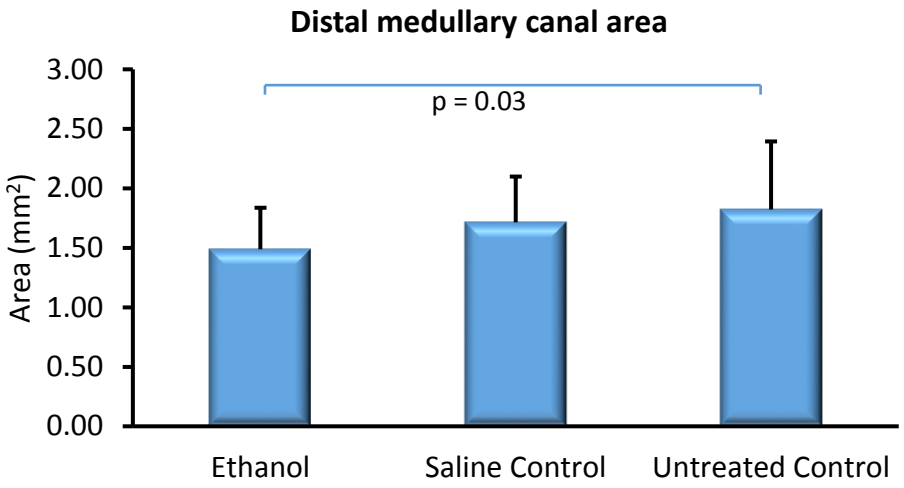

Figure 3.14: Distal medullary canal area. The mean medullary canal area at the 75th percentile mark is given for the three groups studied. Error bars represent standard deviation, and a line connects group with significance difference from the ethnaol group.

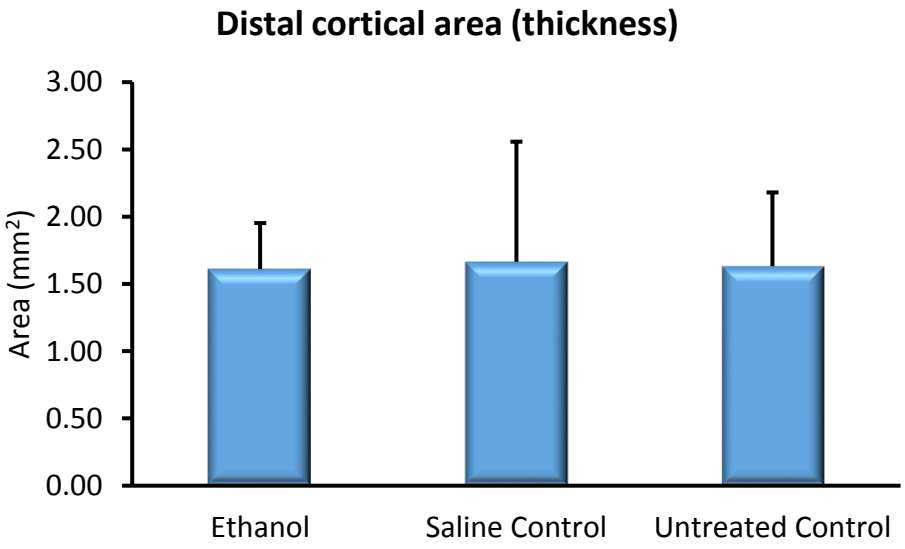

Figure 3.15: Distal cortical area. The mean cortical area at the 75th percentile mark is given for the three groups studied. Error bars represent standard deviation.

3.7.4 Relationship of cross-sectional area with cortical thickness and medullary thickness

In the midshaft, the cross-sectional area for the ethanol group was highly correlated with the medullary canal area (R=0.612, p=0.002) and cortical thickness (R=0.784, p=<0.001) (Table 3.2). This pattern of high correlation also occurred in the saline group with the midshaft cross sectional area being correlated with the medullary canal area (R=0.849, p=<0.001) and cortical thickness (R=0.942, p=<0.001) (Table 3.2).

In the distal region, the cross-sectional area for the ethanol group was also highly correlated with the medullary canal area (R=0.854, p=<0.001) and cortical thickness (R=0.833, p=<0.001) (Table 3.2). A similar pattern was observed in the saline control medullary canal area (R=0.782, p=<0.001) and cortical thickness (R=0.742, p=<0.001) (Table 3.2).

Table 3.2: Pearson's correlation of cross sectional area with cortical thickness and medullary thickness in the ethanol group and saline controls

		Ethanol		**Saline Control**	
		Medullary Canal Area	Cortical Thickness	Medullary Canal Area	Cortical Thickness
Midshaft Cross Sectional Area	Correlation	0.612	0.784	0.849	0.942
	p value	0.002	<0.001	<0.001	<0.001
	N	22	22	21	21
Distal Cross-Sectional Area	Correlation	0.854	0.833	0.782	0.742
	p value	<0.001	<0.001	<0.001	<0.001
	N	22	22	24	24

3.7.5 Relationship of osteometric and trabecular morphometric parameters

In the ethanol group, full bone length was highly correlated with shaft length (R=0.864, <0.001) and distal volume (R=0.723, p=0.002) (Table 3.3). This high correlation of full bone length with shaft length (R=0.788, <0.001) and distal volume (R=0.534, p=0.001) was also observed in the saline control group (Table 3.4). There was no correlation of either full bone or shaft length with trabecular properties in both the ethanol and saline group (Table 3.3). However, shaft length was correlated with distal volume in both the ethanol (R = 0.664, p =0.005) and saline control group (R = 0.447, p =0.032) (Table 3.4).

There was also a strong correlation of distal volume with bone to total volume ratio (BV/TV) (R=0.731, p=0.002) and thickness (TbTh) (R=0.840, p=0.032) in the ethanol group (Table 3.3). This pattern of correlation of distal volume with bone to total volume ratio (BV/TV) (R=0.731, p=0.002) and trabecular thickness (TbTh) (R=0.747, p<0.001) also occurred in the saline controls (Table 3.4). However, in the ethanol group, the distal volume was negatively correlated with trabecular number (TbN) (R=-0.777, p<0.001) (Table 3.3). On the other hand, the saline group showed that trabecular thickness (TbTh) (R=0.747, p<0.001) and trabecular were also correlated (TbN) (R=0.450, p<0.031) (Table 3.4).

Table 3.3: Pearson's correlation of osteometric as well as trabecular morphometric parameters in the ethanol group.

		Full Bone Length	Shaft Length	Distal Volume	BV/TV Distal	TbTh Distal	TbN Distal	TbSp Distal
Full Bone Length	Correlation	1	0.864	0.723	0.370	0.459	-0.424	-0.283
	P value		<0.001	0.002	0.174	0.086	0.116	0.306
	N	16	16	16	15	15	15	15
Shaft Length	Correlation	0.864	1	0.664	0.388	0.426	-0.319	-0.193
	P value	<0.001		0.005	0.153	0.114	0.246	0.492
	N	16	16	16	15	15	15	15
Distal Volume	Correlation	0.723	0.664	1	0.731	0.840	-0.777	-0.241
	P value	0.002	0.005		0.002	<0.001	0.001	0.386
	N	16	16	16	15	15	15	15
BV/TV Distal	Correlation	0.370	0.388	0.731	1	0.739	-0.615	-0.238
	P value	0.174	0.153	0.002		<0.001	0.004	0.327
	N	15	15	15	20	20	20	19
TbTh Distal	Correlation	0.459	0.426	0.840	0.739	1	-0.840	-0.458
	P value	0.086	0.114	<0.001	<0.001		<0.001	0.049
	N	15	15	15	20	20	20	19
TbN Distal	Correlation	-0.424	-0.319	-0.777	-0.615	-0.840	1	0.385
	P value	0.116	0.246	0.001	0.004	<0.001		0.104
	N	15	15	15	20	20	20	19
TbSp Distal	Correlation	-0.283	-0.193	-0.241	-0.238	-0.458	0.385	1
	P value	0.306	0.492	0.386	0.327	0.049	0.104	
	N	15	15	15	19	19	19	19

Table 3.4: Pearson's correlation of osteometric and trabecular morphometric parameters in the saline controls.

		Full Bone Length	Shaft Length	Distal Volume	BV/TV Distal	TbTh Distal	TbN Distal	TbSp Distal
Full Bone Length	Correlation	1	0.788	0.534	-0.413	-0.419	0.000	0.003
	P value		<0.001	0.011	0.056	0.052	0.999	0.988
	N	22	22	22	22	22	22	22
Shaft Length	Correlation	0.788	1	0.447	-0.286	-0.179	0.152	0.029
	P value	<0.001		0.032	0.186	0.414	0.489	0.896
	N	22	24	23	23	23	23	23
Distal Volume	Correlation	0.534	0.447	1	0.293	0.053	0.274	0.089
	P value	0.011	0.032		0.174	0.810	0.206	0.687
	N	22	23	23	23	23	23	23
BV/TV Distal	Correlation	-0.413	-0.286	0.293	1	0.747	0.348	0.137
	P value	0.056	0.186	0.174		<0.001	0.104	0.533
	N	22	23	23	23	23	23	23
TbTh Distal	Correlation	-0.419	-0.179	0.053	0.747	1	0.450	0.269
	P value	0.052	0.414	0.810	<0.001		0.031	0.214
	N	22	23	23	23	23	23	23
TbN Distal	Correlation	0.000	0.152	0.274	0.348	0.450	1	-0.126
	P value	0.999	0.489	0.206	0.104	0.031		0.567
	N	22	23	23	23	23	23	23
TbSp Distal	Correlation	0.003	0.029	0.089	0.137	0.269	-0.126	1
	P value	0.988	0.896	0.687	0.533	0.214	0.567	
	N	22	23	23	23	23	23	23

3.8 Prediction of group membership using the cortical and medullary canal areas

A binary logistic regression analysis was conducted to predict membership to either the ethanol or saline control group using cortical area (thickness) and medullary canal area as predicting variables. A test of the full model against a constant only model was statistically significant, indicating that the predictors as a set reliably distinguished between ethanol and saline control group membership (Chi square = 17.608, p = 0.007 with df = 6). Nagelkerke's R^2 of 0.487 indicated a moderately strong relationship between prediction and grouping. The Wald criterion demonstrated that only the distal medullary canal area made a significant contribution to prediction of group membership (p =0.0120 (Table 3.5). Prediction success overall was 74.4% (72.7% for the ethanol group and 76.2% saline controls (Table 3.6).

Table 3.5: Cortical and medullary canal area variables in the equation.

Variables in the Equation

	B	S.E.	Wald	df	Sig.	Exp(B)
Midshaft Medullary Area	0.219	2.774	0.006	1	0.937	1.244
Midshaft Cortical Thickness	3.955	3.691	1.148	1	0.284	52.196
Distal Medullary Area	4.576	1.814	6.365	1	0.012	97.161
Distal Cortical Thickness	-3.544	2.786	1.618	1	0.203	0.029
Constant	-0.422	2.608	0.026	1	0.872	0.656

Table 3.6: Group membership classification from cortical and medullary canal area variables.

Classification Table				
Observed		Predicted		
		Group		Percentage Correct
		Ethanol	Saline Control	
Group	Ethanol	16	6	72.7
	Saline Control	5	16	76.2
Overall Percentage				74.4

3.9 Prediction of group membership using the trabecular morphometric parameters

A binary logistic regression analysis was conducted to predict membership to either the ethanol or saline control group using bone volume to total volume ratio, trabecular thickness, number and separation as predicting variables. A test of the full model against a constant only model was statistically significant, indicating that the predictors as a set reliably distinguished between ethanol and saline control group membership (Chi square = 23.748, $p < 0.001$ with df = 4). Nagelkerke's R^2 of 0.577 indicated a moderately strong relationship between prediction and grouping. The Wald criterion demonstrated that only trabecular spacing (TbSp) predict membership (Table 3.7). Prediction success overall was 78.6% (84.2% for the ethanol group and 73.9% saline controls) (Table 3.8).

Table 3.7: Trabecular morphometric variables in the equation.

Variables in the Equation

	B	S.E.	Wald	Df	Sig.	Exp(B)
BV/TV Distal	10.212	6.094	2.808	1	0.094	27238.4
TbTh Distal	7.822	10.542	0.551	1	0.458	2494.944
TbN Distal	0.685	0.423	2.619	1	0.106	1.984
TbSp Distal	41.665	16.795	6.155	1	0.013	12438520
Constant	-14.685	5.475	7.194	1	0.007	0

Table 3.8: Group membership classification from trabecular morphometric parameters.

Classification Table

Observed		Predicted		
		Group		Percentage Correct
		Ethanol	Saline Control	
Group	Ethanol	16	3	84.2
	Saline Control	6	17	73.9
Overall Percentage				78.6

4 DISCUSSION

4.1 Rat model of fetal alcohol syndrome

In the current study, a model of moderate binge drinking was utilized. This model is appropriate in the South African context as reports exist in the literature showing that some women tend to take massive amounts of alcohol within a short duration (binge drinking) (Conover and Jones, 2012). This is due to the stigma associated with alcohol consumption by females in certain communities. The high level of basic health illiteracy also contributes to alcohol intake during pregnancy although many women stop drinking once they know that they are pregnant.

The use of untreated control intends to rule out the potential effects of stress as treatment was through oral gavage, which may elevate stress levels and possibly affect pregnancy. Daily dosing of ethanol mimic regular binge drinking. As alcohol has more calories than rat feed, we expected the ethanol treated animals to either gain more weight than controls or to consume less food or both. However, we found that weight gain and food consumption were similar in all three study groups.

While the level of blood alcohol was elevated, as measured an hour following treatment, a major concern was that rats metabolize alcohol faster than humans as the peak blood ethanol concentration in rodents occurs an hour after administration. Normal blood alcohol levels are exhibited two hours after treatment (Snow and Keiver, 2007). The dosing frequency effectively means that the fetus would be exposed to alcohol for a

limited time (approximately 2 hours) daily. This could potentially impact on the ability to induce gestational alcohol exposure effects.

We chose a dose of 25.2% ethanol in light of the fact that a lower dose could potentially fail to induce the intended effect on the offspring. A higher dose could increase the risk of failed implantations and spontaneous abortions. Reports suggest that prenatal alcohol may result in still births, self-abortion and resorption, and this may result in fewer pups born in the ethanol group (Abel and Dintcheff, 1978; Simpson et al., 2005; Snow and Keiver, 2007). In the present study, no significant differences were observed in litter size and gestation duration although the ethanol group had fewer pups. This suggests that the dose and frequency of ethanol administration employed in this study did not produce any observable effect on the gestation duration and litter size due to lack of statistical significance observed among the groups.

4.2 Prenatal alcohol exposure effects on distal tibia growth plate

Growth plate surface area

Alcohol has been shown to cause changes in the growth plate resulting in a delay in bone development (Miralles-Flores and Delgado-Baeza, 1992). In agreement with this, the growth plate exhibited a smaller surface area in comparison with the controls in the present study. It is possible that the smaller growth plate area in the alcohol group may be a contributing factor in the delayed growth in FAS children.

Proliferative zone surface area and cell count

In the proliferative zone of the growth plate, we found both fewer cells and a smaller surface area in the ethanol treated group compared to the saline and untreated controls. As the growth plate is responsible for longitudinal growth (Nilsson and Baron, 2004; Lui et al., 2011), this could be one of the reasons for the shorter stature exhibited by children with FAS. Miralles-Flores and Delgado-Baeza (1992) investigated the effects of gestational alcohol exposure on 0 and 15 day postnatal pups. Changes in the growth plate were only shown on the later but not on the former. However, Snow and Keiver (2007) found that gestational alcohol affected pups that were surgically removed at 21 days of gestation. Our results corroborate the report of Snow and Keiver (2007). This could be attributed to the duration of alcohol exposure. In their study, alcohol was adminitered three weeks before gestation and three weeks during preganacy.

The ethanol group exhibited fewer cell number and proliferating chondrocytes when compared with the untreated group. The mechanisms in which alcohol affects the proliferative cells are unknown. It is possible that alcohol disturbs cell chondrocyte proliferation in one or more of the cell division phases, resulting in slow proliferation rate. Another possibility is induction of apoptosis, due to a potential DNA damage caused by the teratogenic effects of alcohol or by impaired hormonal regulation of bone metabolism. Further studies are required to ascertain these theories.

Hypertrophic zone surface area and cell count

The hypertrophic zone comprises chondrocytes that are older and larger than the chondrocytes found in the proliferative zone. The more mature cells are located closer to the diaphyseal end of the plate. In the hypertrophic zone, lipids, glycogen, and alkaline phosphatase accumulate, resulting in the calcification of the cartilaginous matrix. The longitudinal growth of bone is a result of cellular division in the proliferative zone along with the maturation of cells in the hypertrophic zone. Although no significant differences were observed between the cell count and the surface area of the hypertrophic zone, differences have been documented in studies by Snow and Keiver (2007), which showed an increase in the surface area of the hypertrophic zone. Differences in findings could be attributed to the ages of the rat pups used, our study reported on the tibial length of postnatal 3 week old pups in comparison to previous reports, in these studies the rat pups were aged 21 day gestation and 0 as well as 15 days postnatal, respectively (Miralles-Flores and Delgado-Baeza, 1992; Snow and Keiver, 2007). The ethanol group exhibited less Ki-67 labelled cells and proliferating chondrocytes when compared with the saline and the untreated groups. The differences noted may be attributed to the same factors that might have affected the cellular proliferation in the proliferative zone.

The differences reported may also have been due to differences in the ages of the rats, since the regulation of bone development varies between pre and postnatal development. Likewise, this may be attributed to the effect of *in utero* ethanol exposure on the expression of local growth factors and systemic hormones which affect osseous tissue development differently during pre and postnatal periods. Furthermore,

differences between the duration of alcohol exposure in the studies may account for the differences reported in the hypertrophic zone. It is clear that research in this area is limited with only two studies focusing on the effects of prenatal alcohol on longitudinal growth. Insight into how the epiphyseal plate is affected by gestational alcohol could provide valuable information in paving the way for appropriate treatment regimens to combat this devastating impact on growth.

4.3 Osteometric and bone internal morphology

Bone length

The full and shaft length of the tibia were similar among all three groups in the study. In contrast, previous studies found shorter tibiae in the ethanol group (Miralles-Flores and Delgado-Baeza, 1992; Simpson et al., 2005; Snow and Keiver, 2007). In the present study, we used 25.2% ethanol whereas other researchers used a higher ethanol concentration of 36% (Miralles-Flores and Delgado-Baeza, 1992; Simpson et al., 2005; Snow and Keiver, 2007). The effects of prenatal ethanol exposure on bone are dose dependent as Simpson et al. (2005) and Snow and Keiver. (2007) showed that 36% ethanol has more adverse effects on bone than 25% and 15% ethanol administered in gestation. A possibility exists that we could have found a shorter length had we used a higher concentration such as 36%.

The gestation duration in our study could have contributed to the similar bone lengths we observed as we allowed the dams to litter naturally resulting in a gestation range of 19-24 days. However, there was no statistical significance in gestation duration in our

study. Other researchers controlled for variation in gestation duration by surgically removing the pups at 21 days gestation. Since treatment was stopped at gestation day 19, some litters may have had an intrauterine recovery period between end of treatment and term (birth) (Miralles-Flores and Delgado-Baeza, 1992; Snow and Keiver, 2007).

Considering the relatively high rate of alcohol metabolism in rats, these animals in our study were only exposed to ethanol for approximately 2 hours per day, as that is the time it takes for rodents to metabolise ethanol (Simpson et al., 2005; Snow and Keiver, 2007). This, combined with the moderate dose of 25.2% ethanol could have possibly spared the animals from more noticeable effects.

These results could potentially be different in humans as most people who drink during pregnancy are less educated and also have lower socioeconomic status, which impacts their diet (May et al., 2013). As the animals were on a nutritious balanced diet, and this could have mitigated the effects of ethanol. Additionally, there was a 3-week postnatal period of no ethanol exposure which may have improved the chances of recovery in some respects such as bone length. Spohr et al. (1993) and Streissguth et al. (1991) suggested that that there is potential for catch up growth following prenatal exposure to ethanol. This proposition requires further studies to establish the facts.

Trabecular bone

In the present study, we found both lower bone volume to total volume (BV/TV) and trabecular thickness (TbTh) to be lower in the ethanol group in comparison with the controls. This finding is similar to previous reports using growing rats (Sampson et al.,

1996; Sampson et al., 1997) and in adult rats (Diamond et al., 1989; Wezeman et al., 1999; Turner et al., 2001; Maddalozzo et al., 2009) showing that alcohol intake reduces trabecular bone volume and aids trabecular thinning. Children with FAS have a higher risk of osteoporosis (Jones and Dwyer, 2000b; Cooper et al., 2001). Osteoporosis is a skeletal disease, characterised by reduction in bone mass and disruption of trabecular and compact bone structure, resulting in loss of mechanical strength and an increased fracture risk (Soares et al., 2010). These features are observed in alcohol fed rats (Wezeman et al., 1999; Hogan et al., 1997) and in young, growing rats (Sampson et al., 1996). Similarly, Chen et al. (2001) found a decrease in trabecular number in the hamster femur following alcohol consumption. This is thought to be due to a decrease in the osteoblast number and size as previously reported in alcohol exposed rats (Diez et al., 1997).

Having not seen differences in bone length among the three groups, we queried whether a size estimation method that includes more dimensions would yield the same observations. Linear measurements such as length are in a single dimension and as such tend to exclude size information from other dimensions in three-dimensional space. We then calculated the distal volume (part below the growth plate), as this is the portion rich in trabeculae. We found that the distal volume was significantly less in the ethanol group compared to the controls despite similar bone lengths. This finding suggests that alcohol affects the distal volume.

The trabecular number (TbN) was not affected in our study. This is similar to the findings of Maddalozzo et al. (2009), who did not find any changes on the TbN in the distal tibial

epiphysis. In their study, 4 weeks old rats were fed over a period of 3 month with 35%. The abnormality may be associated with alcohol induced caloric restriction in their study. There was more trabecular spacing in the ethanol group. This, considered together with the lower BV/TV and TbTh suggests that, although the bone length was similar in all groups, the internal morphology was not the same among the study groups. This indicates that prenatal alcohol exposure at our dosage may affect internal architecture while sparing the external bone length. This disruption of the internal bone morphology may also explain why FAS children are prone to osteoporosis and fracture as they may have less bony material internally.

Cortical thickness and medullary canal area

Cortical bone is the most important factor of bone strength (Maurel et al., 2012). Two studies evaluated the deleterious effect of alcohol intake on cortical bone of rodents. These studies presented negative alterations on the thickness and porosity of the bone (Hogan et al., 1997; Maurel et al., 2012).

4.4 Parameters most affected by prenatal ethanol exposure

Employing a binary logistic regression showed that the distal medullary canal area and trabecular spacing were the main parameters that determined group membership into either ethanol treated or saline control. This means that these two parameters (distal medullary canal area and trabecular spacing) are affected the most in gestational alcohol exposure.

Our finding of a positive correlation between medullary canal area and cortical thickness indicates that the smaller medullary canal was coupled with thinner cortical bone. We propose that this may potentially explain weaker bones observed in FAS children.

The negative correlation of trabecular thickness and spacing in the ethanol group indicates that thin trabecular occurred with more spacing in between. This would contribute to bone weakness. Our findings add light to the question of how osteoporosis and subsequent propensity to fracture may occur in prenatal alcohol exposure.

4.5 Conclusion

Gestational alcohol exposure had an adverse effect on the proliferating chondrocytes that resulted to the reduction in size and surface area of both the proliferative and hypertrophic zones. This may be how diminished stature of the offspring occurs. Fewer proliferative cells were found using the anti-Ki67 antibody, indicating that in utero alcohol exposure slows cell proliferation, contributing to the small stature.

Logistic regression showed that the distal medullary canal area and trabecular separation were the main parameters affected the most by gestational alcohol. The negative correlation of trabecular thickness and spacing in the ethanol group may be a contributor to bone weakness. These findings add new knowledge to how *in utero* alcohol exposure affects the offspring.

4.6 Limitations of the study

Endocrine parameters that control bone formation such as parathyroid hormone have not been included in the study. Our study excluded bone strength parameters due to the

time constraints. The untreated group had a smaller sample size which affected the analysis.

4.7 Recommendations

In this work, more questions have been raised form the available findings. It would therefore be of great importance to further characterise these findings. More work should be put in place to evaluate a specific mechanism by which prenatal alcohol exposure can result to pre and postnatal growth retardation. Understanding this mechanism would be helpful in predicting the effects of various alcohol concentration on pre and postnatal growth development following *in utero* exposure, as well as other teratogenic agents. Areas of interest would be via the direct and indirect mechanisms that control bone growth and development as well as other immunological mechanisms (receptor-mediated and regulation of cellular metabolism). Answers to these questions would help to substantiate the findings in this work and would provide the knowledge that is still lacking today.

APPENDICES

Appendix 1: Turnitin report

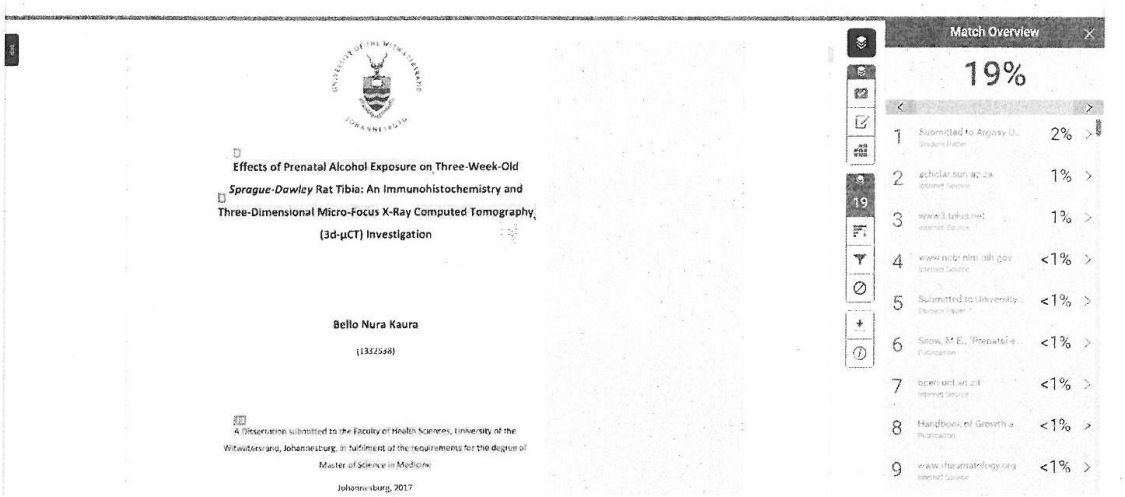

APPENDIX 2: Ethical clearance certificate

STRICTLY CONFIDENTIAL

ANIMAL ETHICS SCREENING COMMITTEE (AESC)

CLEARANCE CERTIFICATE NO. 2015/07/27/C

APPLICANT: Dr R Ndou

SCHOOL: School of Anatomical Sciences
DEPARTMENT:
LOCATION:

PROJECT TITLE: Effects of intrauterine ethanol exposure on skeletal elements in rats (Sprague Dawley)

Number and Species

84 Sprague Dawley Rats (Males and Females)

Approval was given for the use of animals for the project described above at an AESC meeting held on 2015/07/28. This approval remains valid until 2017/09/02.

The use of these animals is subject to AESC guidelines for the use and care of animals, is limited to the procedures described in the application form and is subject to any additional conditions listed below:

None

Signed: _____ (Chairperson, AESC) Date: 10th SEPT 2015

I am satisfied that the persons listed in this application are competent to perform the procedures therein, in terms of Section 23 (1) (c) of the Veterinary and Para-Veterinary Professions Act (19 of 1982)

Signed: _____ (Registered Veterinarian) Date: 10 September 2015

cc: Supervisor: N/A
Director: CAS

Works 2000/lain0015/AESCCert.wps

Appendix 3: Preparation of 10% neutral buffered formalin (10% NBF)

For 1000mls

1. Measure 900mls of distilled water
2. Add 9g of NaCl
3. Add 12g of Na_2HPO_4
4. Place in a beaker and stir using magnetic stirrer until clear
5. Add 10ml of formalin
6. Store at room temperature

Appendix 4: Determination of blood ethanol concentration

1. Dilute samples with assay buffer (1:10 dilution) in a clean test tubes.
2. Prepare Reaction Mix (46µl Ethanol assay buffer, 2µl Ethanol probe, and 2µl Ethanol Enzyme Mix)
3. Add 50µl of the Reaction Mix to all the test tubes
4. Incubate for 60 minutes at room temperature in a dark environment.
5. Measure O.D. 570nm
6. Correct background (difference of background value derived from the 0 ethanol control from all the samples)
7. Calculate ethanol concentration from the standard curve, multiplied by the dilution factor.

   C = Sa/Sv nmol/µl or mM

   Where: **Sa** = sample amount from the Standard Curve (nmol)

   Sv = sample volume added into the samples (µl)

   Ethanol molecular weight: 46.07g/mol

Appendix 5: Tissue decalcification

Methods

1. Put tissue samples in cassettes and immerse in slowly running tap water for 30 minutes
2. Put tissue samples in EDTA for 3 weeks
3. Put tissue sections in running tap water for 30 minutes

Appendix 6: Decalcification end point

Methods

1 Take 5mls of EDTA in to separate test tube
2. Add 10mls ammonium oxalate
3. Mix well and allow to stand overnight
4. Examine for precipitate
5. Repeat if there is precipitate until when clear
6. Rinse in running tap water if no precipitate

Appendix 7: Tissue Processing

The tissue was processed using an automatic tissue processor (Shandon citadel 1000) as follows:

1. 10% buffered formalin for 4 hours
2. 70% alcohol for 1 hour
3. 95% alcohol for 2 hours
4. 95% alcohol for 2 hours
5. 95% alcohol for 2 hours
6. 95% alcohol for 2 hours
7. 100% alcohol for 2 hours
8. 100% alcohol for 2 hours
9. 100% alcohol for 2 hours
10. Chloroform for 2 hours
11. Chloroform for 2 hours
12. Wax for 2 hours
13. Wax for 2 hours

Appendix 8: Paraffin embedding

1. Warm the wax as well as the metal molds and a pair of forceps making sure that the temperature does not exceed 60^{o}C.
2. Once the wax has melted, fill the metal mold with wax.
3. Using the warmed forcep, gently orient the specimens such that the anterior surface of the distal end faces the floor of the mold.
4. Cool briefly, and then cover with the plastic cassette accordingly.
5. Quickly top up with more melted wax and cool for approximately 20 minutes.
6. Separate the metal mold from the plastic cassette.

Appendix 9: Silane coated slides

APES solution

1. 3-aminopropytriethoxysilane 4mls
2. Acetone 200mls

Methods

1. Immerse slides in APES solution
2. Rinse 2x in acetone for 10 dips
3. Rinse 2x in distilled water for 10 dips
4. Air dry at angle of 45 degrees
5. Incubate at 37 degrees overnight

Appendix 10: Staining of tissue sections

Appendix 10.1: Haematoxylin and eosin staining

Haematoxylin solution

For 1000mls

1. Haematoxylin 1g
2. Aluminium potassium sulphate (Potassium alum) 50g
3. Sodium iodate 0.2g
4. Citric acid 1g
5. Chlorate hydrate 50g
6. Allow haematoxylin, alum and sodium iodate to dissolve overnight.
7. Add chloral hydrate and citric acid
8. Boil solution for 5 minutes and then allow to cool.

Eosin solution

For 1000mls

1. Measure 1000mls of distilled
2. Add 8g of stock eosin
3. Add 2g of erythron
4. Stir using a magnetic stirrer

Methods

Hydration

1. Dewax in xylene for 2x10 minutes.
2. Immerse in 2 changes of 100% ethanol for 3 minutes each
3. Immerse in 95% ethanol for 3 minutes
4. Immerse in 70% ethanol for 3 minutes
5. Wash in distilled water for 5 minutes

Nuclear staining

1. Stain with Mayer's haematoxylin for 10 minutes
2. Wash in running tap water for 2 minutes
3. Differentiate in 1% acid alcohol for 2 dips
4. Wash in running tap water for 2 minutes
5. Blue in Scott's tap water for 2 minutes
6. Wash in running tap water for 2 minutes

Cytoplasm staining

1. Stain in eosin for 2 minutes
2. Wash briefly in running tap water

Dehydration and mounting

1. Immerse in 70% ethanol for 3 minutes
2. Immerse in 90% ethanol for 10 minutes
3. Immerse in 100% ethanol for 10 minutes
4. Clear in 2 changes of xylene
5. Mount in entellen

Results

Nuclei: Blue-black

Muscle fibers: deep pinky red

Cytoplasm: Varying shades of pink.

Appendix 10.2: Scott's tap water solutions

For 100mls

1. Sodium hydrogen carbonate 2g
2. Magnesium sulphate 20g
3. Distilled water 1000mls

Dissolve the salts in the water and store in stock solutions at room temperature.

Appendix 10.3: Immunohistochemistry

Sodium citrate buffer (pH 6.0) solution

For 100ml

Tri- sodium citrate (dehydrate).	2.9g
Distilled water	1000ml

Mix to dissolve sodium citrate and adjust pH to 6 with 1ml HCl

Tween 20	0.5ml

Phosphate buffer (pH=7.0) solution

For 2000ml

NaCl	16g
Na_2HPO_4	3.5g
KCl	0.4g
KH_2PO_4	0.4g
Distilled water	2000ml

DAB working solution

DAB chromogen	50µl
Substrate (hydrogen peroxide)	250µl

Primary antibody (Ki-67) dilution factor 1:1200

Phosphate buffer	1200µl
Ki-67	1µl

Remove 1 µ from phosphate buffer and replace with 1200µl of Ki-67 antibody

Methods

Day 1

1. Deparaffinise sections in xylene for 2x 10 minutes
2. Rehydrate sections through graded alcohols
3. Wash slides in running tap water for 5 minutes
4. Antigen retrieve sections in citrate buffer PH 6 (water bath) overnight at 60^{o}

Day 2

5. Allow to cool at room temperature for 20 minutes
6. Wash slides in running tap water for 5 minutes
7. Block endogenous peroxidase with 1% H_2O_2 in methanol for 10 minutes
8. Wash in phosphate buffer solution (PBS) (PH 7.4) for 3x 5 minutes
9. Incubate with normal goat serum 5% (protein block) for 10 minutes
10. Tap serum off slides and wash in PBS for 3x 5 minutes
11. Incubate with primary antibody (Ki-67 1:1200) over night at 4^{o}C

Day 3

12. Allow sections to reach room temperature for 20 minutes
13. Wash in PBS (pH=7.4) for 3x 5 minutes
14. Incubate with biotinylated secondary antibody 3x 5 minutes
15. Wash in PBS for 3x 5 minutes
16. Incubate with Strep Avidin HRP for 10 minutes
17. Wash in PBS for 3x 5 minutes
18. Incubate with DAB working solution for 5 minutes
19. Rinse in running tap water for 5 minutes
20. Blue with Scott's tap water for 2 minutes
21. Wash in running tap water for 5 minutes
22. Hydrate through graded alcohol
23. Clear in xylene and mount with entellen

Appendix 11: Cells count

1. Import image in to image J (file > open)
2. Go to image on the software and click on image > type > 8 bit
3. Click on process > subtract background and adjust pixel size to 12
4. Click on image > adjust > threshold > apply
5. Click on process > binary > fill holes
6. Click on process > binary > convert to mask
7. Click on process > binary > watershed
8. Click on polygonal selection tool and demarcate region of interest
9. Click on analyse > analyse particles
10. Select bare outline and summarise result on the popped up window
11. Click “OK”

Appendix 12: Measurement of cortical thickness

1. Import image (file > open
2. Select line tool and draw a line along the entire length of the scale bar
3. Select analyse > set scale
4. Type the known distance 2 and the unit of length (mm) in the box that appeared
5. Check on the global and click “OK”
6. Select analyse > tools > ROI manager. A window will appear
7. Select polygonal selection tool
8. Delineate the cross sectional area
9. Click add on the ROI manager
10. Delineate the medullary area
11. Click add on the ROI manager
12. Click measure and calculate the difference

REFERENCES

Abel E, Dintcheff B. 1978. Effects of prenatal alcohol exposure on growth and development in rats. The Journal of Pharmacology and Experimental Theurapeutics 207:916-921.

Allen MR, Hock JM, Burr DB. 2004. Periosteum: biology, regulation, and response to osteoporosis therapies. Bone 35:1003-1012.

Apte SS. 1990. Expression of the cell proliferation-associated nuclear antigen reactive with the Ki-67 monoclonal antibody by cells of the skeletal system in humans and other species. Bone and Mineral 10:37-50.

Ballock RT, O'keefe RJ. 2003. The biology of the growth plate. American Journal of Bone and Joint Surgery 85:715-726.

Barbier A, Martel C, De Vernejoul M, Tirode F, Nys M, Mocaer G, Morieux C, Murakami H, Lacheretz F. 1999. The visualization and evaluation of bone architecture in the rat using three-dimensional X-ray microcomputed tomography. Journal of Bone and Mineral Metabolism 17:37-44.

Beto JA. 2015. The role of calcium in human aging. Clinical Nutrition Research 4:1-8.

Bonnet N, Laroche N, Vico L, Dolleans E, Courteix D, Benhamou C. 2009. Assessment of trabecular bone microarchitecture by two different x-ray microcomputed tomographs: a comparative study of the rat distal tibia using Skyscan and Scanco devices. Medical Physics 36:1286-1297.

Boskey AL, Coleman R. 2010. Aging and bone. Journal of Dental Research 89:1333-1348.

Bouchery EE, Harwood HJ, Sacks JJ, Simon CJ, Brewer RD. 2011. Economic costs of excessive alcohol consumption in the US, 2006. American Journal of Preventive Medicine 41:516-524.

Bouxsein ML, Boyd SK, Christiansen BA, Guldberg RE, Jepsen KJ, Müller R. 2010. Guidelines for assessment of bone microstructure in rodents using micro–computed tomography. Journal of Bone and Mineral Research 25:1468-1486.

Brommage R. 2003. Validation and calibration of DEXA body composition in mice. American Journal of Physiology-Endocrinology and Metabolism 285:454-459.

Brown D, Gatter K. 1990. Monoclonal antibody Ki-67: its use in histopathology. Histopathology 17:489-503.

Bruno S, Darzynkiewicz Z. 1992. Cell cycle dependent expression and stability of the nuclear protein detected by Ki-67 antibody in HL-60 cells. Cell Proliferation 25:31-40.

Carter D, Van der Meulen M, Beaupre G. 1996. Mechanical factors in bone growth and development. Bone 18:5-10.

Carvalho ICS, Dutra TP, De Andrade DP, Balducci I, Pacheco-Soares C, Rocha RFd. 2016. High doses of alcohol during pregnancy cause DNA damages in osteoblasts of newborns rats. Birth Defects Research Part A: Clinical and Molecular Teratology 106:122-132.

Castania VA, Silveira JWdSd, Issy AC, Pitol DL, Castania ML, Neto AD, Del Bel EA, Defino HLA. 2015. Advantages of a combined method of decalcification compared to EDTA. Microscopy Research and Technique 78:111-118.

Chakkalakal D, Novak J, Fritz E, Mollner T, McVicker D, Lybarger D, McGuire M, Donohue T. 2002. Chronic ethanol consumption results in deficient bone repair in rats. Alcohol and Alcoholism 37:13-20.

Chakkalakal DA. 2005. Alcohol-induced bone loss and deficient bone repair. Alcoholism: Clinical and Experimental Research 29:2077-2090.

Chang G. 2001. Alcohol screening instruments for pregnant women. Alcohol Research and Health 25:204-209.

Chang G, Goetz MA, Wilkins-Haug L, Berman S. 2000. A brief intervention for prenatal alcohol use An in-depth look. Journal of Substance Abuse Treatment 18:365-369.

Chappard D, Retailleau-Gaborit N, Legrand E, Baslé MF, Audran M. 2005. Comparison insight bone measurements by histomorphometry and µCT. Journal of Bone and Mineral Research 20:1177-1184.

Chavassieux P, Serre CM, Vergnaud P, Delmas PD, Meunier PJ. 1993. In vitro evaluation of dose-effects of ethanol on human osteoblastic cells. Bone and Mineral 22:95-103.

Chen H, Hayakawa D, Emura S, Ozawa Y, Taguchi H, Yano R, Shoumura S. 2001. Effects of ethanol on the ultrastructure of the hamster femur. Histology and Histopathology 16:763-770.

Christiansen BA, Bouxsein ML. 2013. Assessment of bone mass and microarchitecture in rodents. Primer on the Metabolic Bone Diseases and Disorders of Mineral Metabolism 1:38-45.

Chudley AE, Conry J, Cook JL, Loock C, Rosales T, LeBlanc N. 2005. Fetal alcohol spectrum disorder: Canadian guidelines for diagnosis. Canadian Medical Association Journal 172:1-21.

Clarke B. 2008. Normal bone anatomy and physiology. Clinical Journal of the American Society of Nephrology 3:131-139.

Conover E, Jones K. 2012. Safety concerns regarding binge drinking in pregnancy: a review. Birth Defects Research: Part A, Clinical and Molecular Teratology 94:570-575.

Cooper C, Eriksson J, Forsen T, Osmond C, Tuomilehto J, Barker D. 2001. Maternal height, childhood growth and risk of hip fracture in later life: a longitudinal study. Osteoporosis International 12:623-629.

Croxford J, Viljoen D. 1999. Alcohol consumption by pregnant women in the Western Cape. South African Medical Journal 89:962-965.

Day NL. 1992. The effects of prenatal exposure to alcohol. Alcohol Research and Health 16:238-244.

Dempster DW. 2000. The contribution of trabecular architecture to cancellous bone quality. Journal of Bone and Mineral Research 15:20-23.

Diamond T, Stiel D, Lunzer M, Wilkinson M, Posen S. 1989. Ethanol reduces bone formation and may cause osteoporosis. The American Journal of Medicine 86:282-288.

Diez A, Serrano S, Cucurull J, Mariñoso L, Bosch J, Puig J, Nogués X, Aubia J. 1997. Acute effects of ethanol on mineral metabolism and trabecular bone in sprague-dawley rats. Calcified Tissue International 61:168-171.

Dwek JR. 2010. The periosteum: what is it, where is it, and what mimics it in its absence? Skeletal Radiology 39:319-323.

Elledge SJ. 1996. Cell cycle checkpoints: preventing an identity crisis. Science 274:1664-1672.

Eriksen EF. 2010. Cellular mechanisms of bone remodeling. Reviews in Endocrine and Metabolic Disorders 11:219-227.

Ernhart C, Wolf A, Linn P, Sokol R, Kennard M, Filipovich H. 1985. Alcohol related birth defects, syndromal anomalies,intrauterie growth retardation, and neonatal behavioral assessment. Alcoholism: Clinical and Experimental Research 9:447-453.

Ethen MK, Ramadhani TA, Scheuerle AE, Canfield MA, Wyszynski DF, Druschel CM, Romitti PA. 2009. Alcohol consumption by women before and during pregnancy. Maternal and Child Health Journal 13:274-285.

Fajardo RJ, Cory E, Patel ND, Nazarian A, Laib A, Manoharan RK, Schmitz JE, DeSilva JM, MacLatchy LM, Snyder BD. 2009. Specimen size and porosity can introduce error into μCT-based tissue mineral density measurements. Bone 44:176-184.

FitzHarris G. 2012. Anaphase B precedes anaphase A in the mouse egg. Current Biology 22:437-444.

Friday KE, Howard GA. 1991. Ethanol inhibits human bone cell proliferation and function in vitro. Metabolism 40:562-565.

Genant HK, Jiang Y. 2006. Advanced imaging assessment of bone quality. Annals of the New York Academy of Sciences 1068:410-428.

Gerdes J, Lemke H, Baisch H, Wacker H-H, Schwab U, Stein H. 1984. Cell cycle analysis of a cell proliferation-associated human nuclear antigen defined by the monoclonal antibody Ki-67. The Journal of Immunology 133:1710-1715.

Gibson LJ. 1985. The mechanical behaviour of cancellous bone. Journal of Biomechanics 18:317-328.

Gilbert SF, 2000. Developmental Biology, 6th ed Sunderland (MA), Sinauer Associates.

Godfrey K, Walker-Bone K, Robinson S, Taylor P, Shore S, Wheeler T, Cooper C. 2001. Neonatal bone mass: influence of parental birthweight, maternal smoking, body composition, and activity during pregnancy. Journal of Bone and Mineral Research 16:1694-1703.

Gong Z, Wezeman FH. 2004. Inhibitory effect of alcohol on osteogenic differentiation in human bone marrow–derived mesenchymal stem cells. Alcoholism: Clinical and Experimental Research 28:468-479.

Hahn M, Vogel M, Pompesius-Kempa M, Delling G. 1992. Trabecular bone pattern factor—a new parameter for simple quantification of bone microarchitecture. Bone 13:327-330.

Hall P, Levison D. 1990. Assessment of cell proliferation in histological material. Journal of Clinical Pathology 43:184-192.

Hartwell LH, Weinert TA. 1989. Checkpoints: controls that ensure the order of cell cycle events. Science 246:629-634.

Heby O. 1981. Role of polyamines in the control of cell proliferation and differentiation. Differentiation 19:1-20.

Hildebrand T, Rüegsegger P. 1997. A new method for the model-independent assessment of thickness in three-dimensional images. Journal of Microscopy 185:67-75.

Hitchcock CL. 1991. Ki-67 staining as a means to simplify analysis of tumor cell proliferation. American Journal of Clinical Pathology 96:444-447.

Hogan H, Sampson H, Cashier E, Ledoux N. 1997. ALcohol consumption by young actively growing rats: a study of cortical bone histomorphometry and mechanical properties. Alcoholism: Clinical and Experimental Research 21:809-816.

Horvitz HR, Herskowitz I. 1992. Mechanisms of asymmetric cell division: two Bs or not two Bs, that is the question. Cell 68:237-255.

Howlett C. 1979. The fine structure of the proximal growth plate of the avian tibia. Journal of Anatomy 128:377-399.

Hunziker EB. 1994. Mechanism of longitudinal bone growth and its regulation by growth plate chondrocytes. Microscopy Research and Technique 28:505-519.

Jan YN, Jan LY. 1998. Asymmetric cell division. Nature 392:775-778.

Jiang Y, Zhao J, White D, Genant H. 2000. Micro CT and Micro MR imaging of 3D architecture of animal skeleton. Journal of Musculoskeletal and Neuronal Interactions 1:45-51.

Jones G, Dwyer T. 2000. Birth weight, birth length, and bone density in prepubertal children: evidence for an association that may be mediated by genetic factors. Calcified Tissue International 67:304-308.

Kapadia RD, Stroup GB, Badger AM, Koller B, Levin JM, Coatney RW, Dodds RA, Liang X, Lark MW, Gowen M. 1998. Applications of micro-CT and MR microscopy to study pre-clinical models of osteoporosis and osteoarthritis. Technology and Health Care 6:361-372.

Keiver K, Ellis L, Anzarut A, Weinberg J. 1997. Effect of prenatal ethanol exposure on fetal calcium metabolism. Alcoholism: Clinical and Experimental Research 21:1612-1618.

Keiver K, Herbert L, Weinberg J. 1996. Effect of maternal ethanol consumption on maternal and fetal calcium metabolism. Alcoholism: Clinical and Experimental Research 20:1305-1312.

Keiver K, Weinberg J. 2004. Effect of duration of maternal alcohol consumption on calcium metabolism and bone in the fetal rat. Alcoholism: Clinical and Experimental Research 28:456-467.

Kierszembaum AL, Tres LL, 2012. Histology and cell biology: an introduction to pathology, 3rd ed. Philadelphia, PA: Saunders

King RW, Jackson PK, Kirschner MW. 1994. Mitosis in transition. Cell 79:563-571.

Konishi T, Takeyasu A, Natsume T, Furusawa Y, Hieda K. 2011. Visualization of heavy ion tracks by labeling 3'-OH termini of induced DNA strand breaks. Journal of Radiation Research 52:433-440.

Labib M, Abdel-Kader M, Ranganath L, Teale D, Marks V. 1989. Bone disease in chronic alcoholism: the value of plasma osteocalcin measurement. Alcohol and Alcoholism 24:141-144.

Landberg G, Tan EM, Roos G. 1990. Flow cytometric multiparameter analysis of proliferating cell nuclear antigen/cyclin and Ki-67 antigen: a new view of the cell cycle. Experimental Cell Research 187:111-118.

Larkby C, Day N. 1997. The effects of prenatal alcohol exposure. Alcohol Research and Health 21:192-198.

Lui J, Nilsson O, Barona J. 2011a. Growth plate senescence and catch-up growth. Endocrine Development 21:23-29.

Lundsberg LS, Bracken MB, Saftlas AF. 1997. Low-to-moderate gestational alcohol use and intrauterine growth retardation, low birthweight, and preterm delivery. Annals of Epidemiology 7:498-508.

LuValle P, Beier F. 2000. Cell cycle control in growth plate chondrocytes. Frontiers in Bioscience 5:493-503.

Mackie E, Ahmed Y, Tatarczuch L, Chen K-S, Mirams M. 2008. Endochondral ossification: how cartilage is converted into bone in the developing skeleton. The International Journal of Biochemistry and Cell Biology 40:46-62.

Maddalozzo GF, Turner RT, Edwards CH, Howe KS, Widrick JJ, Rosen CJ, Iwaniec UT. 2009. Alcohol alters whole body composition, inhibits bone formation, and increases bone marrow adiposity in rats. Osteoporosis international 20:1529-1538.

Maurel D, Boisseau N, Benhamou C, Jaffre C. 2012. Cortical bone is more senstive to alcohol dose effects than trabecular bone in the rat. Bone 79:492-499.

May P, Blankenship J, Marais A-S, Gossage J, Kalberg W, Barnard R, De Vries M, Robinson L, Adamns C, Buckley D, Manning M, Jones K, Parry C, Hoyme H, Seedat S. 2013. Approaching the prevalence of the full spectrum of fetal alcohol spectrum disorders in a South African population-based study. Alcoholism: Clinical and Experimental Research 37:818-830.

May PA, Baete A, Russo J, Elliott AJ, Blankenship J, Kalberg WO, Buckley D, Brooks M, Hasken J, Abdul-Rahman O. 2014. Prevalence and characteristics of fetal alcohol spectrum disorders. Pediatrics 134:855-866.

May PA, Gossage JP. 2001. Estimating the prevalence of fetal alcohol syndrome: A summary. Alcohol Research and Health 25:159-167.

May PA, Gossage JP, Kalberg WO, Robinson LK, Buckley D, Manning M, Hoyme HE. 2009. Prevalence and epidemiologic characteristics of FASD from various research methods with an emphasis on recent in-school studies. Developmental Disabilities Research Reviews 15:176-192.

May PA, Gossage JP, Marais A-S, Adnams CM, Hoyme HE, Jones KL, Robinson LK, Khaole NC, Snell C, Kalberg WO. 2007. The epidemiology of fetal alcohol syndrome and partial FAS in a South African community. Drug and Alcohol Dependence 88:259-271.

McCormick D, Chong H, Hobbs C, Datta C, Hall P. 2002. Detection of the Ki-67 antigen in fixed and wax-embedded sections with the monoclonal antibody MIB1. Histopathology 41:173-178.

Medina AE. 2011. Fetal alcohol spectrum disorders and abnormal neuronal plasticity. The Neuroscientist 17:274-287.

Miralles-Flores C, Delgado-Baeza E. 1992. Histomorphometric analysis of the epiphyseal growth plate in rats after prenatal alcohol exposure. Journal of Orthopaedic Research 10:325-336.

Nagy TR, Clair AL. 2000. Precision and accuracy of dual-energy X-ray absorptiometry for determining in vivo body composition of mice. Obesity 8:392-398.

Nilsson O, Baron J. 2004. Fundamental limits on longitudinal bone growth:growth plate senescence and epiphyseal fusion. Trends in Endocrinology and Metabolism 15:370-374.

Nurse P. 1994. Ordering S phase and M phase in the cell cycle. Cell 79:547-550.

Nwaogu I. 2002. Growth rate of bones in rat foetal alcohol syndrome. Veterinarski Archive 72:343-351.

O'Leary CM. 2004. Fetal alcohol syndrome: diagnosis, epidemiology, and developmental outcomes. Journal of Paediatrics and Child Health 40:2-7.

Olegård R, SABEL KG, Aronsson M, Sandin B, Johansson P, Carlsson C, Kyllerman M, Iversen K, Hrbek A. 1979. Effects on the child of alcohol abuse during pregnancy: retrospective and prospective studies. Acta Paediatrica 68:112-121.

Olivier L, Curfs L, Viljoen D. 2016. Fetal alcohol spectrum disorders: Prevalence rates in South Africa. South African Medical Journal 106:103-106.

Ornoy A, Ergaz Z. 2010. Alcohol abuse in pregnant women: effects on the fetus and newborn, mode of action and maternal treatment. International Journal of Environmental Research and Public Health 7:364-379.

Ortega N, Behonick DJ, Werb Z. 2004. Matrix remodeling during endochondral ossification. Trends in Cell Biology 14:86-93.

Pattern A, Fontaine C, Christie B. 2014. A comparison of the different animal models of fetal alcohol spectrum disorders and their use instudying complex behaviors. Frontiers in Pediatrics 2:1-19.

Peng TC, Lian JB, Hirsch PF, Kusy RP. 1991. Lower serum osteocalcin in ethanol-fed rats. Journal of Bone and Mineral Research 6:107-115.

Percival CJ, Richtsmeier JT. 2013. Angiogenesis and intramembranous osteogenesis. Developmental Dynamics 242:909-922.

Ramadoss J, Hogan HA, Given JC, West JR, Cudd TA. 2006. Binge alcohol exposure during all three trimesters alters bone strength and growth in fetal sheep. Alcohol 38:185-192.

Ramos-Vara J. 2005. Technical aspects of immunohistochemistry. Veterinary Pathology Online 42:405-426.

Rho J-Y, Kuhn-Spearing L, Zioupos P. 1998. Mechanical properties and the hierarchical structure of bone. Medical Engineering and Physics 20:92-102.

Riley EP, Infante MA, Warren KR. 2011. Fetal alcohol spectrum disorders: an overview. Neuropsychology Review 21:73-80.

Roach HI, Erenpreisa J, Aigner T. 1995. Osteogenic differentiation of hypertrophic chondrocytes involves asymmetric cell divisions and apoptosis. The Journal of Cell Biology 131:483-494.

Roozen S, Peters GJY, Kok G, Townend D, Nijhuis J, Curfs L. 2016. Worldwide Prevalence of Fetal Alcohol Spectrum Disorders: A Systematic Literature Review Including Meta-Analysis. Alcoholism: Clinical and Experimental Research 40:18-32.

Rosenthal J, Christianson A, Cordero J. 2005. Fetal alcohol syndrome prevention in South Africa and other low-resource countries. American Journal of Public Health 95:1099-1101.

Rüegsegger P, Koller B, Müller R. 1996. A microtomographic system for the nondestructive evaluation of bone architecture. Calcified Tissue International 58:24-29.

Salic A, Mitchison TJ. 2008. A chemical method for fast and sensitive detection of DNA synthesis in vivo. Proceedings of the National Academy of Sciences 105:2415-2420.

Sampson HW, Chaffin C, Lange J, DeFee B, 2nd. 1997. Alcohol consumption by young actively growing rats: a histomorphometric study of cancellous bone. Alcoholism: Clinical and Experimental Research 21:352-359.

Sampson HW, Perks N, Champney TH, DeFee B, 2nd. 1996. Alcohol consumption inhibits bone growth and development in young actively growing rats. Alcoholism: Clinical and Experimental Research 20:1375-1384.

Sasaki K, Murakami T, Kawasaki M, Takahashi M. 1987. The cell cycle associated change of the Ki-67 reactive nuclear antigen expression. Journal of Cellular Physiology 133:579-584.

Schafer K. 1998. The cell cycle: a review. Veterinary Pathology 35:461-478.

Scholzen T, Gerdes J. 2000. The Ki-67 protein: from the known and the unknown. Journal of Cellular Physiology 182:311-322.

Shapiro F. 2008. Bone development and its relation to fracture repair. The role of mesenchymal osteoblasts and surface osteoblasts. European Cells and Materials 15:53-76.

Shi S-R, Cote RJ, Taylor CR. 2001. Antigen retrieval techniques Current perspectives. Journal of Histochemistry and Cytochemistry 49:931-937.

Simpson M, Duggal S, Keiver K. 2005. Prenatal alcohol exposure has differential effects on fetal growth and skeletal ossification. Bone 36:521-532.

Snow M, Keiver K. 2007. Prenatal ethanol exposure disrupts the histological stages of fetal bone development. Bone 41:181-187.

Soares EA, Favaro WJ, Cagnon VHA, Bertran CA, Camilli JA. 2010. Effects of alcohol and nicotine on the mechanical resistance of bone and bone neoformation around hydroxyapatite implants. Journal of Bone Mineral Metabolism 28:101-107.

Sokol RJ, Miller SI, Reed G. 1980. Alcohol abuse during pregnancy: an epidemiologic study. Alcoholism: Clinical and Experimental Research 4:135-145.

Spohr H, Willis J, Steinhausen.HC. 1993. Prenatal alcohol exposure and long term developmental cosequences. Lancet 341:907-910.

Stevens DA, Williams GR. 1999. Hormone regulation of chondrocyte differentiation and endochondral bone formation. Molecular and Cellular Endocrinology 151:195-204.

Streissguth A, Aase J, Clarren S, Randels S, LaDue R, Smith D. 1991. Fetal alcohol syndrome in adolscents and adults. Journal American Medical Association 265:1961-1967.

Turner R, Kidder L, Kennedy A, Evans G, Sibonga J. 2001. Moderate alcohol consumption suppress bone turnover in adults female rats. Journal of Bone and Mineral Research 16:589-594.

Urban M, Chersich MF, Fourie L-A, Chetty C, Olivier L, Viljoen D. 2008. Fetal alcohol syndrome among grade 1 schoolchildren in Northern Cape Province: prevalence and risk factors. South African Medical Journal 98:877-882.

Viguet-Carrin S, Garnero P, Delmas P. 2006. The role of collagen in bone strength. Osteoporosis International 17:319-336.

Viljoen DL, Gossage JP, Brooke L, Adnams CM, Jones KL, Robinson LK, Hoyme HE, Snell C, Khaole NC, Kodituwakku P. 2005. Fetal alcohol syndrome epidemiology in a South African community: a second study of a very high prevalence area. Journal of Studies on Alcohol 66:593-604.

Waarsing JH, Day JS, Weinans H. 2004. An improved segmentation method for in vivo µCT imaging. Journal of Bone and Mineral Research 19:1640-1650.

Warren KR, Calhoun FJ, May PA, Viljoen DL, Li TK, Tanaka H, Marinicheva GS, Robinson LK, Mundle G. 2001. Fetal alcohol syndrome: an international perspective. Alcoholism: Clinical and Experimental Research 25:202-206.

Wehrli FW. 2007. Structural and functional assessment of trabecular and cortical bone by micro magnetic resonance imaging. Journal of Magnetic Resonance Imaging 25:390-409.

Weiner S, Wagner HD. 1998. The material bone: structure-mechanical function relations. Annual Review of Materials Science 28:271-298.

Wezeman FH, Emanuele M, Emanuele N, MoskolII S, Woods W, Suri M, Steiner J, Lapaglia N. 1999. Chronic alcohol consumption during male rat adolescence impairs skeletal development through effects on oteoblast gene expression, bone mineral density and bone strength. Alcoholism: Clinical and Experimental Research 23:1534-1542.

Wezeman FH, Gong Z. 2004. Adipogenic Effect of Alcohol on Human Bone Marrow-Derived Mesenchymal Stem Cells. Alcoholism: Clinical and Experimental Research 28:1091-1101.

Wilkins B. 1992. Histology of normal haemopoiesis: bone marrow histology. Journal of Clinical Pathology 45:645-649.

Wilsman NJ, Farnum CE, Green EM, Lieferman EM, Clayton MK. 1996. Cell cycle analysis of proliferative zone chondrocytes in growth plates elongating at different rates. Journal of Orthopaedic Research 14:562-572.

Windham GC, Fenster L, Hopkins B, Swan SH. 1995. The association of moderate maternal and paternal alcohol consumption with birthweight and gestational age. Epidemiology 6:591-597.

Winey M, Mamay CL, O'toole ET, Mastronarde DN, Giddings TH, McDonald KL, McIntosh JR. 1995. Three-dimensional ultrastructural analysis of the Saccharomyces cerevisiae mitotic spindle. The Journal of Cell Biology 129:1601-1615.

Yu CC-W, Woods AL, Levison DA. 1992. The assessment of cellular proliferation by immunohistochemistry: a review of currently available methods and their applications. The Histochemical Journal 24:121-131.

Zakhari S, Li TK. 2007. Determinants of alcohol use and abuse: impact of quantity and frequency patterns on liver disease. Hepatology 46:2032-2039.